学位論文

Theoretical study on volume law of Rényi entanglement entropy in quantum many-body systems

(量子多体系におけるレニー・エンタングルメントエントロピーの体積則に関する理論的研究)

平成 29 年 12 月博士 (理学) 申請

東京大学大学院 理学系研究科
物理学専攻

中川裕也

Abstract

Thermal equilibrium in quantum many-body systems can be fully described by pure quantum states as far as local observables are concerned, while the conventional description of it is based on mixed-state ensembles. The thermodynamic entropy, in that case, is identified with the entanglement entropy of small subsystems. It scales with the size of the subsystem, which is called the volume law of entanglement. When the size of the subsystem increases, however, the correspondence between thermal and entanglement entropies fails and there appears a quantum correction to the simple volume-law scaling. Explicating the scaling of the entanglement entropy with the subsystem size is hence of great importance in connecting quantum physics to thermodynamics as well as analyzing recent experiments on ultracold atoms. In this thesis, we study the volume law of entanglement for pure quantum states representing thermal equilibrium. We derive an analytic formula of the volume law of entanglement for a certain class of pure states called canonical Thermal Pure Quantum (cTPQ) states which represent thermal equilibrium. We illustrate an advantage of the formula by numerically calculating the entanglement entropy of the cTPQ states and applying the formula to it. Furthermore, we argue that our formula universally applies to any sufficiently *scrambled* pure state, even if the state is not thermal. We consider two examples of such scrambled states, namely, stationary pure states after quantum quench and energy eigenstates of general Hamiltonians with and without integrability. The entanglement entropy of the former states, including actual experimental data in ultracold atoms, is in an excellent agreement with our formula as long as the states are scrambled. For the latter states, we find that our formula works as a good fitting function in non-integrable models to extract information in the thermodynamic limit from finite size systems. We also show that our formula can distinguish eigenstates of integrable models from non-integrable ones.

List of publications and preprints

1. "Flux quench in a system of interacting spinless fermions in one dimension", Yuya O. Nakagawa, Grégoire Misguich, and Masaki Oshikawa, Phys. Rev. B **93**, 174310 (2016).

2. "Fractional quantum Hall states of dipolar fermions in a strained optical lattice", Hiroyuki Fujita, Yuya O. Nakagawa, Yuto Ashida, and Shunsuke Furukawa, Phys. Rev. A **94**, 043641 (2016).

3. "Universality in volume law entanglement of pure quantum states", Hiroyuki Fujita, Yuya O. Nakagawa, Sho Sugiura, and Masataka Watanabe, arXiv:1703.02993.

4. "Construction of Hamiltonians by machine learning of energy and entanglement spectra", Hiroyuki Fujita, Yuya O. Nakagawa, Sho Sugiura, and Masaki Oshikawa, arXiv:1705.05372 (accepted in Phys. Rev. B).

5. "Numerical calculations on the relative entanglement entropy in critical spin chains", Yuya O. Nakagawa and Tomonori Ugajin, J. Stat. Mech. **(2017)** 093104.

6. "Capacity of entanglement and the distribution of density matrix eigenvalues in gapless systems", Yuya O. Nakagawa and Shunsuke Furukawa, Phys. Rev. B **96**, 205108 (2017).

This thesis is based on the result in the preprint 3.

Contents

Chapter 1

Introduction

In this chapter, we introduce notions which are central to the contents of this thesis. In the first two sections, we review two different backgrounds of this study: entanglement in quantum many-body systems and thermodynamics in terms of pure states. Then in the following sections we present the main theme of this thesis, the volume law scaling of the entanglement for thermal pure states, and explain a purpose and motivations of this study.

1.1 Entanglement in quantum many-body systems

Quantum entanglement lies at the heart of quantum mechanics. It was firstly noticed by Einstein-Podolsky-Rosen [1] and Schrödinger [2] as a phenomenon where some composite systems cannot be written as a product of its subsystems, which implies the existence of hidden non-local correlations in quantum systems beyond the classical mechanics. One consequence of this "spooky" feature of quantum mechanics was formulated as the violation of Bell's inequality [3], and it was experimentally verified by a series of experiments in quantum optics [4–6]. Since the 1990's, quantum entanglement has played a crucial role in quantum information science and its applications [7,8], such as quantum computation, quantum teleportation, and quantum cryptography.

Recently, entanglement has also become an important tool to study quantum many-body systems in condensed matter physics as well as high-energy physics. By calculating entanglement measures in the many-body wave function $|\psi\rangle$, one can tell various properties of a system [9, 10]. The most famous and celebrated measure among them is the von Neumann entanglement entropy (vN-EE). With a bipartition of the system into a subregion A and its complement B, the vN-EE is defined as

$$S_{EE} := -\operatorname{tr}_A (\rho_A \ln \rho_A) , \tag{1.1}$$

which is the von Neumann entropy of the reduced density matrix (RDM) on the subsystem A,

$$\rho_A := \operatorname{tr}_B |\psi\rangle \langle\psi| . \tag{1.2}$$

Another important measure of the entanglement is the n-th Rényi entanglement entropy

(nREE), defined as

$$S_n := \frac{1}{1-n} \ln \left(\mathrm{tr}_A \, \rho_A^n \right). \tag{1.3}$$

This is a one-parameter generalization of the vN-EE and has properties

$$\lim_{n \to 1} S_n = S_{EE}, \tag{1.4}$$

$$S_n \geq S_{n'} \quad \text{for} \quad n < n'. \tag{1.5}$$

Moreover, the REEs including the vN-EE are symmetric under the exchange of the subsystems $A \leftrightarrow B$,

$$\rho_B := \mathrm{tr}_A \left| \psi \right\rangle \left\langle \psi \right|, \;\; \mathrm{tr}_B \, \rho_B^n = \mathrm{tr}_A \, \rho_A^n \quad \text{for} \; \forall n. \tag{1.6}$$

From the viewpoint of quantum many-body systems, these EEs (the vN-EE and REE) are interesting in that (i) they cannot be expressed as expectation values of a single operator, i.e. "non-linear" quantities, and (ii) they are highly non-local when the size of the subsystem is comparable with that of the total system. Therefore the EEs have a potential to reveal properties of quantum many-body systems which cannot be detected by conventional (linear and local) observables. While the EEs were featured on the theoretical side at first, state-of-the-art techniques can now measure them experimentally in ultracold atoms, trapped ions, superconducting qubits, and nuclear spins of molecules [11–16], which fuels further growing interest among both theorists and experimentalists.

In particular, when the state $|\psi\rangle$ is a ground state of local Hamiltonian[1], there are a lot of studies about the entanglement properties in the literature. The scaling of the EEs of the ground state is known to obey the "area law" of entanglement. That is, the EEs scale with the boundary size of A with a possible logarithmic correction [17, 18],

$$S_n \sim \alpha_1 \, \ell^{d-1} \ln \ell + \alpha_2 \, \ell^{d-1} + \cdots, \tag{1.7}$$

where we take the subsystem A as a d-dimensional ball-like region of a linear dimension ℓ, for simplicity. The specific form of the scaling can reflect universal numbers characterizing the system or the presence of certain nontrivial correlations. For example, in one-dimensional quantum critical systems, the REE for a subsystem of length ℓ exhibits the (area law) logarithmic scaling $S_n = \frac{(n+1)c}{6n} \ln \frac{\ell}{a}$, where c and a are the central charge and the (non-universal) short-distance cutoff of underlying conformal field theory [19–22]. Another example is free fermions and Fermi liquids in general dimensions, where the vN-EE and the REE detect a presence of the Fermi surface through a multiplicative logarithmic correction (the first term of Eq. (1.7)) in the area law [23–28]. Furthermore, in topologically ordered systems the EEs obey the area law with a subleading universal constant that specifies the underlying topological properties which cannot be identified by conventional local observables [29–32].

In contrast to the ground state, excited pure states of local Hamiltonians exhibit another scaling of the entanglement. This is called the "volume law" of entanglement, which states that the amount of entanglement between the subsystems A and B is proportional to the size of the subsystem,

$$S_n \sim \alpha' \, \ell^d + \cdots, \tag{1.8}$$

[1] In this thesis, we mean by **local** that all terms in the Hamiltonian have the support which does not scale with the system size.

where we use the same notation as Eq. (1.7). Compared with the area law for the ground state, the volume law for excited states has not been investigated extensively and its universal behavior (if any) remains an open question. However, the volume law is quite important in that it can bridge quantum mechanics and thermodynamics when one considers the notion of *pure state thermodynamics*. We will introduce this point in the next section.

1.2 Pure state thermodynamics and thermal pure states

Standard textbooks on quantum statistical mechanics teach that a quantum system in thermal equilibrium at an inverse temperature β is described by the following density matrix,

$$\rho_{\text{Gibbs}}(\beta) = \frac{1}{Z(\beta)} e^{-\beta H}, \tag{1.9}$$

where H is the Hamiltonian of the system and $Z(\beta) := \operatorname{tr} e^{-\beta H}$ is the partition function of the system. We call this state as the Gibbs state and stress that the Gibbs states are mixed states[2] except for the ground state, $\beta = \infty$.

Usual justification of the usage of the Gibbs state is based on the postulate of "the equal *a priori* probability". The postulate claims that the state in thermal equilibrium which has energy E is described by an equally-weighted classical superposition of many eigenstates,

$$\rho_{MC}(E) = \frac{1}{N(E)} \sum_{E_i \in \left[E-\frac{\delta}{2}, E+\frac{\delta}{2}\right]} |E_i\rangle \langle E_i| . \tag{1.10}$$

Here the microcanonical (MC) ensemble $\rho_{MC}(E)$ is composed of the energy eigenstates of the system $\{|E_i\rangle\}$, and the normalization constant $N(E)$ is the number of states within the energy shell at the energy E with δ being the width of the energy shell. Let us divide the system into the subsystem of interest, A, and the bath, B, and decompose the Hamiltonian of the total system into the Hamiltonian on each subsystem and the interactions between them, $H = H_A + H_B + H_{\text{int}}$. When the subsystem B is quite large[3] compared with A, one obtains

$$\operatorname{tr}_B \left(\rho_{MC}(E)\right) \approx \rho_{\text{Gibbs},A}(\beta_E) := \frac{1}{Z_A(\beta_E)} e^{-\beta_E H_A}, \tag{1.11}$$

where $Z_A(\beta) := \operatorname{tr}_A e^{-\beta H_A}$. The temperature β_E is determined by the microcanonical entropy of the system[4] $S(E) = \ln N(E)$ through the relation $\beta_E = \frac{\partial S(E)}{\partial E}$. This is how

[2] The density matrix (or the quantum state) ρ is called mixed when there is no vector $|\phi\rangle$ in the Hilbert space that satisfies $\rho = |\phi\rangle\langle\phi|$. This condition is equivalent to $\operatorname{tr}\rho^2 < 1$.

[3] In this statement, we consider the thermodynamic limit where the size of the subsystem B becomes infinite while keeping the size of the subsystem A finite. The same thermodynamic limit is considered also in Eq. (1.12).

[4] Strictly speaking, $S(E)$ is the microcanonical entropy of the subsystem B. Here we assume translational invariance in the total system.

the Gibbs state is derived in the standard ensemble formalism of quantum statistical mechanics based on the postulate of the equal *a priori* probability.

However, the very assumption of the equal *a priori* probability has been debated for a long time, and construction of thermodynamics with only using *pure quantum states* has been considered as early as the age of von Neumann [33, 34]. Recently, a series of studies based on "typicality" [35–41] revealed that the postulate actually can be abandoned and that one can take another more natural principle. Instead of taking the MC ensemble $\rho_{MC}(E)$ (mixed state), one can randomly choose a pure state $|\phi_E\rangle$ in the energy shell of the total system at the energy E, and it follows almost surely that

$$\mathrm{tr}_B \left(|\phi_E\rangle \langle \phi_E| \right) \approx \rho_{\mathrm{Gibbs},A}(\beta_E), \tag{1.12}$$

as long as the bath (subsystem B) is by far larger than the subsystem A. In other words, almost all pure states $|\phi_E\rangle$ in the energy shell give the same physical consequences as the MC ensemble does, as long as the subsystem A is much smaller than the subsystem B. In this sense, one can think of the pure state thermodynamics under the "typicality principle": typical pure states in the Hilbert space represent the thermal equilibrium.

Motivated by the above discussion on the pure state thermodynamics, in this thesis we focus on "thermal pure states" which is defined as follows.

Definition. *When a given pure state $|\psi\rangle$ satisfies the following property for all local*[5] *operators $\mathcal{O}$ in the Hilbert space, we call $|\psi\rangle$ as a thermal pure state at inverse temperature β,*

$$\frac{\langle \psi | \mathcal{O} | \psi \rangle}{\langle \psi | \psi \rangle} = \mathrm{tr} \left(\mathcal{O} \rho_{\mathrm{Gibbs}}(\beta) \right). \tag{1.13}$$

Clearly, typical pure states in the Hilbert space satisfy the above condition and can be considered as thermal pure states because one can take the support of the operator $\mathcal{O}$ as the subsystem A in the previous paragraph. Although we have so far introduced the thermal pure states from a conceptual (or purely-theoretical) aspect, there are actually several situations where it is inevitable to consider them rather than the conventional mixed-state ensemble. One of the examples is the thermalization in closed quantum systems that is discussed in detail in section 3.1. If a given initial state of the system, say the universe, is pure, then the unitary time-evolution $\rho(t) = U_t^\dagger \rho(0) U_t$ preserves the purity of the system: $\mathrm{tr}\, \rho(t)^2 = \mathrm{tr}\, \rho(0)^2 = 1$. Hence the initial state cannot relax into the mixed-state ensembles, so the thermalization in closed quantum systems must be written in the language of pure states. The dynamics in closed quantum systems has also been realized in experiments during the past decade, for example, in ultracold atoms, trapped ions, and so on [12, 15, 16, 42–49].

1.3 Volume law of entanglement

The difference between the thermal pure states and the mixed-state ensembles, by definition, appears only in non-local quantities in the system. One natural candidate of such

[5] Again we mean by local that the support of the operator does not scale with the size of the total system.

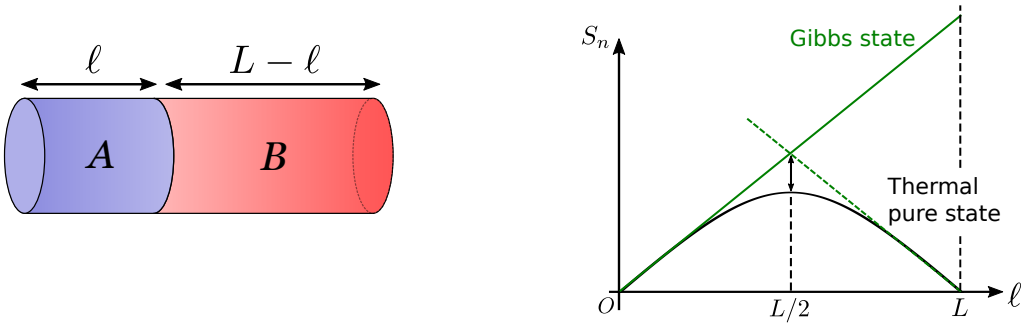

Figure 1.1: A schematic picture of the REE of the thermal pure states and the Gibbs states. (left) We divide the total system into the subsystems A and B whose volumes are parameterized as ℓ and $L-\ell$, respectively. (right) The REE curve $S_n(\ell)$ for thermal pure states (black line) and the Gibbs states (green line). Both curves follow the volume law when ℓ is small, but the former one gradually deviates from it as ℓ grows and takes maximal at the middle ($\ell = L/2$). Past the middle, it decreases toward $\ell = L$ so that the whole curve becomes symmetric under the exchange $\ell \leftrightarrow L-\ell$. In contrast, the latter curve simply grows with ℓ.

quantities is the entanglement which we introduced in section 1.1, and in fact it manifests the difference clearly. Figure 1.1 is a schematic picture of the REE of the thermal pure states and the Gibbs states in translation invariant systems. Here, the REE of the Gibbs states is defined by its RDM on the subsystem A,

$$\sigma_A := \mathrm{tr}_B\left(\rho_{\mathrm{Gibbs}}(\beta)\right), \; S_{n,\mathrm{Gibbs}} := \frac{1}{1-n}\ln\left(\mathrm{tr}_A\,\sigma_A^n\right), \tag{1.14}$$

in the same way as the thermal pure states. For simplicity, we parametrize the volume of the subsystem A as ℓ and the subsystem B as $L-\ell$, so the total size of the system is L. We note that the dimensionality does not matter here. When the subsystem A is much smaller than half of the total system ($\ell \ll L$), the REE of two states scales with the volume of the subsystem ($\propto \ell$, the volume law), and matches with each other because the RDMs of both states are the same (Eqs. (1.11) and (1.12)). However, when the subsystem A is comparable to or larger than the subsystem B, the REE of two states starts to deviate. The REE of the thermal pure states deviates from the volume law $S_n \propto \ell$ around $\ell = L/2$, and decrease after $\ell = L/2$ so as to be symmetric under the exchange of the subsystem $A \leftrightarrow B$. In contrast, the Gibbs states do not have such symmetry and the REE grows linearly[6] as ℓ until it reaches $\ell = L$. Therefore, in the region of $\ell \sim L/2$ and $\ell > L/2$, the REEs of the thermal pure states and the Gibbs states exhibit different behaviors.

The overall functional form the REE curve $S_n(\ell)$ for thermal pure states, which is the main theme of this thesis, has not been elucidated except for the random state that

[6] This is because the REE of the Gibbs states contains contributions from a classical superposition of a huge number of pure states (eigenstates of the system). The amount of entanglement, or quantum correlation, in the Gibbs states must be measured by the mutual information between two subsystems that is known to obey the area law [50].

corresponds to infinite temperature $\beta = 0$. In the seminal paper [51] which has become important for solving the black hole information paradox [52], Page conjectured the shape of the curve for $\ell \leq L/2$ is

$$S_{EE}(\ell) = \left(\sum_{k=d_B+1}^{d_A d_B} \frac{1}{k} \right) - \frac{d_A - 1}{2d_B}, \tag{1.15}$$

where $d_{A(B)}$ is the Hilbert space dimension of the subsystem $A(B)$. When we denote $d_A = \lambda^\ell$ and $d_B = \lambda^{L-\ell}$ with λ being the local dimension of the Hilbert space (in spin $S = 1/2$ systems, for example, $\lambda = 2$) and assume $\ell \gg 1$, the result leads to

$$S_{EE}(\ell) \approx \ell \ln \lambda - \frac{1}{2}\lambda^{-L+2\ell}. \tag{1.16}$$

This conjecture, which was proved afterwards [53–55], tells that the vN-EE deviates from the volume law by $O(e^{-\ell})$ for $1 \ll \ell \ll L/2$ and by exactly $O(1) = \frac{1}{2}$ at $\ell = L/2$. We also note that the nREE of the random state for $\ell \gg 1$ and $L - \ell \gg 1$ was studied in Ref. [56], and the deviation from the volume law is also $O(1)$ for general $n > 0$.

1.4 Motivations and purpose of our study

In this thesis, we will address the following questions.

(1) What is the functional form of the REE curve $S_n(\ell)$ for thermal pure states at finite temperature $0 < \beta < \infty$?

(2) Is the result universal among the thermal pure states?

Indeed, there are a plenty of implications in answering these questions. First, since the REE is a highly non-local and non-linear quantity, revealing the precise behavior of the REE of thermal pure states will contribute to the foundation of the pure state thermodynamics where local and linear observables have been mainly studied. The REE is a fundamental quantity from the theoretical point of view because it would correspond to the entropies of the (thermal) Gibbs states. Particularly, it is interesting to see whether the deviation of $S_n(\ell)$ from the simple volume law ($\propto \ell$) around the center $\ell \sim L/2$ is $O(1)$ or $O(L)$. If the deviation is $O(1)$ (which turns out to be the case as shown in Chapter 2), it means that the density of the REE, $S_n(\ell)/\ell$, is still consistent with that of the thermal ensembles even though the size of the subsystem A is comparable to the rest of the system (= the subsystem B = bath). Second, elucidating properties of entanglement in thermal pure states is important to study the thermalization in closed quantum systems. As we introduced in section 1.2, entanglement plays an important role to make pure states look mixed-state thermal ensembles (because the RDM of a given pure state cannot become mixed if there is no entanglement in the state). In this sense, spreading of entanglement in the whole system is crucial for the thermalization to occur. Thus studying the REE $S_n(\ell)$ of given pure states and comparing it with that of the thermal pure states help to give a criterion of the thermalization. Third, identifying and characterizing parameter(s) in the functional form of the volume-law scaling of thermal pure states would pave the

way to study various (including unconventional) ordered states in quantum many-body systems at finite temperature. This is analogous to the case of the ground state of local Hamiltonians introduced in section 1.1, where the parameters (coefficients, offset) of the area-law scaling diagnose the orders in the ground state of the system. Fourth, a complete characterization of the REE curve $S_n(\ell)$ will be of benefit to the estimation of the slope of the volume law at the small subsystem ($1 \ll \ell \ll L/2$). The slope of the volume law for thermal pure states corresponds to the density of the REEs of the thermal Gibbs ensemble, so it is important for inferring thermodynamic profiles (entropy, free energy, etc.) of the thermal pure states[7]. Actually, the curve like Fig. 1.1 is observed ubiquitously in many theoretical and experimental studies [12, 57–60]. Nevertheless, the available system size L in numerical and experimental studies is often limited to $L \sim 20$, so the estimation of the volume-law slope is deteriorated by the curved structure of the REE curve. Hence the knowledge of the functional form of the curve will be of quite use to improve the analysis of the data.

We mainly focus on the second Rényi entanglement entropy $S_2(\ell)$ in this thesis. One of the reasons for this is because the 2REE is simplest among nREEs ($0 < n < \infty$) to compute theoretically (for example, by the Monte Carlo method [61–63]) and measure experimentally [11, 12, 14, 16]. Another reason is because the 2REE can be related to the out-of-time-order correlators (OTOCs) [64], which are important to study one of the most interesting problems in quantum many-body systems: chaos in quantum systems [65–67]. Here we define the OTOC as

$$F(t) = \langle \hat{W}(t)\hat{V}(0)\hat{W}(t)\hat{V}(0)\rangle_\beta \,,$$

where $\hat{W}(t) = e^{iHt}\hat{W}e^{-iHt}, \hat{V}(t) = e^{iHt}\hat{V}e^{-iHt}$ are some Hermite operators in the system and the expectation value is taken for the thermal ensemble at inverse temperature β. The decay of the OTOC in time implies that the commutator $\langle [\hat{W}(t), \hat{V}(0)]^2\rangle_\beta$ gets large, so it would reflect the chaotic behavior of the system (the butterfly effect). Indeed, the OTOC is expected to decay exponentially in chaotic quantum systems. Ref. [64] showed

$$\exp(-S_2^V(t)) = \sum_{\hat{W}\in B} \langle \hat{W}(t)\hat{V}(0)\hat{W}(t)\hat{V}(0)\rangle_{\beta=0} \,,$$

where $S_2^V(t)$ is the 2REE of the infinite-temperature Gibbs state excited by $\sqrt{\hat{V}}$ at $t = 0$, or $\rho(t) = e^{-iHt}\cdot\sqrt{\hat{V}}\rho_{\text{Gibbs}}(\beta = 0)\sqrt{\hat{V}}\cdot e^{iHt} = e^{-iHt}\hat{V}e^{iHt}$, and the summation is taken over a complete orthonormal set of operators in the subsystem B. This equation states that the decay of (the average of) the OTOC is equivalent to growth of the 2REE, and hence the 2REE can extract information about the chaotic behavior of the system. Although the analytical relation between the OTOC and the 2REE in the above was proved only when the initial state at $t = 0$ is mixed, numerical results in Ref. [64] suggest that the correspondence is also the case for pure states.

[7] Strictly speaking, only the vN-EE ($n = 1$ REE) corresponds to thermal entropy directly. However, if $\text{tr}_B(|\psi\rangle\langle\psi|) = \rho_{\text{Gibbs},A}(\beta)$ holds, the nREE of $|\psi\rangle$ is equal to $\frac{n\beta}{n-1}\left(F_A(n\beta) - F_A(\beta)\right)$, where $F_A(\beta) = -\beta^{-1}\ln\left(\text{tr}_A(e^{-\beta H_A})\right)$ is the free energy of the subsystem A [57]. In addition, since the inequality $S_{EE} = S_1 \geq S_2 \geq \cdots$ holds, the information of the 2REE, 3REE, $\cdots$ gives a lower bound of the (thermal) entropy of the system.

1.5 Organization of this thesis

This thesis is organized as follows. Chapter 2 is dedicated to an analytical derivation of a functional form of the volume law of entanglement for thermal pure states, by using the canonical Thermal Pure Quantum states (the cTPQ states). The cTPQ state is an explicit and analytically-tractable construction of thermal pure states in general systems, and we derive the functional form of the REE curve $S_n(\ell)$ for the cTPQ states. We also deepen the discussion of the volume law and conjecture that our formula will universally apply to general *scrambled* pure quantum states, which include many kinds of thermal pure states other than the cTPQ states. In Chapter 3, we numerically study the conjecture by applying our formula of the volume law to pure states after quantum quench. We observe an excellent agreement of the formula to stationary states after quantum quench, as long as the states are "scrambled". Moreover, we apply the formula to recent experimental data obtained in ultracold atoms [12], and it works quite well. In Chapter 4 we present the application of the formula to another type of thermal pure states: energy eigenstates of general Hamiltonians. As expected, our numerical results seem consistent with the formula in non-integrable systems, whereas it is not the case in integrable systems. However, Lu and Grover [68] recently derived a different functional form of the volume law for energy eigenstates in non-integrable systems. We study this point in detail and claim that our formula is still useful to energy eigenstates in non-integrable systems even though the exact functional form of the volume law in a certain thermodynamic limit does not match with our formula. Finally, the summary and conclusion of this study will be presented in Chapter 5.

Chapter 2

Universal functional form of the volume law of entanglement derived by using canonical Thermal Pure Quantum states

In this chapter, we present an analytical formula of the volume law of entanglement by employing the canonical Thermal Pure Quantum states. First we introduce the cTPQ states and explain their properties. Next we derive the analytical expressions of the n-th REE of the cTPQ states, especially focusing on the second Rényi entanglement entropy (2REE). Interestingly, the formula of the 2REE contains only two parameters and the whole structure of the volume law is determined by them. We also demonstrate that our formula of the volume law has advantages in extracting the entropic density of a system in the thermodynamic limit from numerical data of finite size systems. Finally we conjecture that our functional form will apply to any "scrambled" pure state, which includes a broad class of thermal pure states other than the cTPQ states, based on the discussion in deriving the functional form for the cTPQ states.

2.1 Definition of canonical Thermal Pure Quantum states

Inspired by the studies of the typicality [33–40], Sugiura and Shimizu [41] proposed a class of pure states which reproduce expectation values of the canonical ensemble for any local operator. It is called the canonical Thermal Pure Quantum (cTPQ) states, defined as

$$|\psi_\beta\rangle = \frac{1}{\sqrt{Z(\beta)}} \sum_j z_j e^{-\beta H/2} |j\rangle \,, \tag{2.1}$$

where $Z(\beta) := \mathrm{tr}\left(e^{-\beta H}\right)$ is a partition function of the system, $\{|j\rangle\}_j$ is an arbitrary complete orthonormal basis of the Hilbert space, and the coefficients $\{z_j\}$ are random complex numbers $z_j = (x_j + iy_j)/\sqrt{2}$ with x_j and y_j obeying the standard normal distribution $\mathcal{N}(0,1)$. For any local observable $\mathcal{O}$ in the Hilbert space, random average of the

expectation values by the cTPQ states matches with that of the Gibbs state,

$$\overline{\langle\psi_\beta|\mathcal{O}|\psi_\beta\rangle} = \mathrm{tr}(\mathcal{O}e^{-\beta H})/\,\mathrm{tr}(e^{-\beta H}), \tag{2.2}$$

where random average over the coefficients $\{z_j\}$ is denoted by $\overline{\cdots}$. Moreover, the standard deviation from the average $\sqrt{\overline{\langle\psi_\beta|\mathcal{O}^2|\psi_\beta\rangle} - \left(\overline{\langle\psi_\beta|\mathcal{O}|\psi_\beta\rangle}\right)^2}$ is exponentially small in the volume of the system [41]. In this sense, one can regard the cTPQ states $|\psi_\beta\rangle$ as an explicit example of thermal pure states at inverse temperature β. We note that $|\psi_\beta\rangle$ is normalized only after the random average, $\overline{\langle\psi_\beta|\psi_\beta\rangle} = 1$. It is usually difficult or computationally costly to calculate the normalization factor $Z(\beta)$, but we can use an unnormalized version of the cTPQ states, $|\phi_\beta\rangle = \sum_j z_j e^{-\beta H/2}|j\rangle$, in practice. One can prove $\langle\phi_\beta|\mathcal{O}|\phi_\beta\rangle\,/\,\langle\phi_\beta|\phi_\beta\rangle = \mathrm{tr}(\mathcal{O}e^{-\beta H})/\,\mathrm{tr}(e^{-\beta H})$ and the standard deviation is still small.

The cTPQ states are practically useful because we only need to prepare a single pure state (vector) and apply the Hamiltonian (matrix) to it to calculate physical quantities at finite temperature[1] $T = \beta^{-1} > 0$, whereas computation of them by the Gibbs states requires full diagonalization of the Hamiltonian that costs huge computational resources. Therefore more and more numerical studies in condensed matter physics have employed the cTPQ states recently [69–73].

Since this cTPQ formalism can apply to general systems, we employ the cTPQ states as analytically-tractable thermal pure states which exhibit the volume law of entanglement. In the following section, we derive a functional form of the volume law of entanglement.

2.2 Derivation of a functional form

2.2.1 Exact result of random average

Let us clarify our setup. We consider a lattice Σ containing $L \times M$ sites (left panel of Fig. 1.1) with a local Hamiltonian H. We divide Σ into two subsystems, A and B, each containing $\ell \times M$ and $(L-\ell) \times M$ sites. For simplicity we set $M = 1$, i.e., consider a one-dimensional system throughout this thesis, but our results in this thesis will hold in general dimensions as long as the volumes of the subsystems are parameterized as one-dimensional parameters ℓ and $L - \ell$. We assume translation invariance of the Hamiltonian[2]. In addition, we assume $\ell, L-\ell \gg 1$ to facilitate thermodynamic behaviors of the subsystems (we will see this point later).

As introduced in Chapter 1, the nREE of the cTPQ state $|\psi_\beta\rangle$ is

$$S_n(\ell) = \frac{1}{1-n}\ln\left(\mathrm{tr}_A\,\rho_A^n\right),\ \rho_A = \mathrm{tr}_B\,|\psi_\beta\rangle\langle\psi_\beta|\,. \tag{2.3}$$

[1] Throughout this thesis, we set $k_B = \hbar = 1$.

[2] Precisely speaking, we can loosen the assumption of the translational invariance a little; the translational invariance can be broken on the boundary, i.e., the boundary condition does not matter. This is because we will focus on bulk (extensive) properties of the system and subsystems in derivation of the formula of the volume law. It is enough to assume that the subsystems A and B have the same thermodynamic limit for all bipartitions of the system.

The reduced density matrix ρ_A can be written as

$$\rho_A = \frac{1}{Z(\beta)} \sum_{a_1,a_2,b_1,i_1,j_1} \pi_{12} \left|a_1\right\rangle \left\langle a_2\right|, \tag{2.4}$$

where $\pi_{pq} := z_{i_p} z_{j_p}^* \left\langle a_p b_p | e^{-\frac{1}{2}\beta H} | i_p \right\rangle \left\langle j_p | e^{-\frac{1}{2}\beta H} | a_q b_p \right\rangle$, $|ab\rangle := |a\rangle \otimes |b\rangle$, and $\{|a\rangle\}_a$ and $\{|b\rangle\}_b$ are complete orthonormal bases in the subsystem A and B, respectively. Two indices $i_p, j_q \in \{|j\rangle\}_j$ run over a complete orthonormal basis $\{|j\rangle\}_j$ in the total system. In this notation we obtain

$$\mathrm{tr}_A\, \rho_A^n = \frac{\sum_{(a),(b),(i),(j)} \pi_{12}\pi_{23}\cdots\pi_{n1}}{Z(\beta)^n}, \tag{2.5}$$

where $(x) := x_1, x_2, \cdots, x_n$. What we would like to compute is a random average of n-th REE, $\overline{S_n} := \dfrac{1}{1-n}\overline{\ln\left(\mathrm{tr}_A\, \rho_A^n\right)}$. The term $\pi_{12}\pi_{23}\cdots\pi_{n1}$, however, includes the product of random variables such as $z_{i_1} z_{j_1}^* z_{i_2} z_{j_2}^* \cdots z_{i_n} z_{j_n}^*$ and it is difficult to calculate the average of the *logarithm* of it. Instead, we calculate S_n by averaging the trace before taking the logarithm of it, $\tilde{S}_n := \dfrac{1}{1-n} \ln\left(\overline{\mathrm{tr}_A\, \rho_A^n}\right)$. As we give a proof in appendix A, the difference between $\overline{S}_n$ and $\tilde{S}_n$ is exponentially small in terms of the system size L (see also Ref. [68] for a similar discussion). In the following calculation we just use S_n to denote $\tilde{S}_n$.

Taking the random average of $\mathrm{tr}_A\, \rho_A^n$ can be performed by using several properties of $\{z_i\}$ such as $\overline{z_i} = 0$, $\overline{z_i^* z_j} = \delta_{ij}$ and $\overline{|z_i|^2 |z_j|^2} = 1 + \delta_{ij}$. For example, calculation of the second REE goes like

$$\begin{aligned}
\overline{\mathrm{tr}_A\, \rho_A^2} &= \sum_{\substack{i,j,k,l \\ a_1,b_1,a_2,b_2}} \frac{\overline{z_i z_j^* z_k z_l^*} \left\langle a_1 b_1 | e^{-\beta H/2} | i \right\rangle \left\langle j | e^{-\beta H/2} | a_2 b_1 \right\rangle \left\langle a_2 b_2 | e^{-\beta H/2} | k \right\rangle \left\langle l | e^{-\beta H/2} | a_1 b_2 \right\rangle}{Z(\beta)^2} \\
&= \sum_{a_1,b_1,a_2,b_2} \frac{\left\langle a_1 b_1 | e^{-\beta H} | a_2 b_1 \right\rangle \left\langle a_2 b_2 | e^{-\beta H} | a_1 b_2 \right\rangle + \left\langle a_1 b_1 | e^{-\beta H} | a_1 b_2 \right\rangle \left\langle a_2 b_2 | e^{-\beta H} | a_2 b_1 \right\rangle}{Z(\beta)^2} \\
&= \frac{\mathrm{tr}_A \left(\mathrm{tr}_B\, e^{-\beta H}\right)^2 + \mathrm{tr}_B \left(\mathrm{tr}_A\, e^{-\beta H}\right)^2}{Z(\beta)^2},
\end{aligned} \tag{2.6}$$

which results in

$$S_2 = -\ln\left[\frac{\mathrm{tr}_A \left(\mathrm{tr}_B\, e^{-\beta H}\right)^2 + \mathrm{tr}_B \left(\mathrm{tr}_A\, e^{-\beta H}\right)^2}{Z(\beta)^2}\right]. \tag{2.7}$$

Similarly, the third REE is

$$S_3 = -\frac{1}{2}\ln\left[\frac{\mathrm{tr}_A (\mathrm{tr}_B\, e^{-\beta H})^3 + 3\,\mathrm{tr}\left(e^{-\beta H}\left(\mathrm{tr}_B\, e^{-\beta H} \otimes \mathrm{tr}_A\, e^{-\beta H}\right)\right) + \mathrm{tr}_B \left(\mathrm{tr}_A\, e^{-\beta H}\right)^3 + N}{Z(\beta)^3}\right], \tag{2.8}$$

where $N = \sum_{a_1,a_2,a_3,b_1,b_2,b_3} \left\langle a_1 b_1 | e^{-\beta H} | a_3 b_2 \right\rangle \left\langle a_2 b_2 | e^{-\beta H} | a_1 b_3 \right\rangle \left\langle a_3 b_3 | e^{-\beta H} | a_2 b_1 \right\rangle$. We can calculate the nREE for given integer $n \geq 2$ systematically, but it is difficult to write down

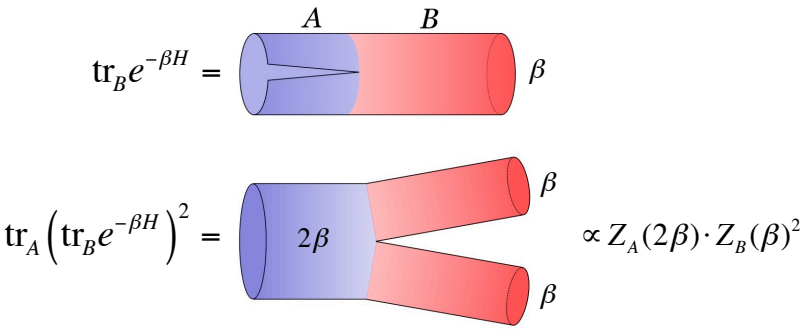

Figure 2.1: Pictorial expression of the approximation $\mathrm{tr}_A(\mathrm{tr}_B\, e^{-\beta H})^2 \propto Z_A(2\beta)Z_B(\beta)^2$. (top) The matrix $\mathrm{tr}_B\, e^{-\beta H}$ can be considered as a cylinder of radius β with a slit on the subsystem A by the Suzuki-Trotter decomposition [74]. The horizontal direction is the spacial dimension and the circumferential direction represents the imaginary time-evolution. (bottom) $\mathrm{tr}_A(\mathrm{tr}_B\, e^{-\beta H})^2$ can be considered as a Y-shaped cylinder. If we neglect the contribution from the boundary between A and B, it is approximated as $Z_A(2\beta)\cdot Z_B(\beta)^2$.

general expressions of it because the calculation of $\overline{\mathrm{tr}_A\,\rho_A^n}$ involves a contraction of $2n$ complex numbers which yields complicated products of the matrix $e^{-\beta H}$. Thus the vN-EE $S_{\mathrm{EE}} = \lim_{n\to 1} S_n = -\mathrm{tr}_A(\rho_A \ln \rho_A)$ has yet to be calculated, and it would be interesting to study it by computing a general formula of S_n and performing the analytic continuation $n \to 1$ to it.

2.2.2 Simplification to a universal functional form of the volume law

It is possible to make several simplifications of Eq. (2.7) under physically-reasonable assumptions. The first step is to decompose the Hamiltonian H as $H = H_A + H_B + H_{\mathrm{int}}$, where $H_{A,B}$ are the Hamiltonians of the corresponding subsystems and H_{int} describes the interactions between them. Since the range of interaction H_{int} is much smaller than ℓ and $L-\ell$ because of the assumption that H is local, we can approximate

$$Z(\beta) \propto Z_A(\beta)Z_B(\beta),\ \mathrm{tr}_B(\mathrm{tr}_A\, e^{-\beta H})^2 \propto Z_A(\beta)^2 Z_B(2\beta),\ \mathrm{tr}_A(\mathrm{tr}_B\, e^{-\beta H})^2 \propto Z_A(2\beta)Z_B(\beta)^2, \tag{2.9}$$

where $Z_{A,B}(\beta) := \mathrm{tr}_{A,B}\,(e^{-\beta H_{A,B}})$ is the partition function of each subsystem and the proportional constants are independent of ℓ and β (we will consider these approximations in detail later). A pictorial understanding of the second and the third approximations is presented in Fig. 2.1. By putting these approximations into Eq. (2.7), one obtains

$$S_2(\ell) = -\ln\left(\frac{Z_A(2\beta)}{Z_A(\beta)^2} + \frac{Z_B(2\beta)}{Z_B(\beta)^2}\right) + \ln R(\beta), \tag{2.10}$$

where $R(\beta)$ is a constant coming from the proportional constants in Eq. (2.7).

Further simplification can be obtained by considering the extensiveness of the free energy, $-\frac{1}{\beta}\ln Z_A \propto \ell$ and $-\frac{1}{\beta}\ln Z_B \propto L-\ell$, which is valid (see also the last paragraph of this subsection) when $\ell,\ L-\ell \gg 1$. We thus replace $Z_A(2\beta)/Z_A(\beta)^2$ and $Z_B(2\beta)/Z_B(\beta)^2$

with $Q(\beta)a(\beta)^{-\ell}$ and $Q(\beta)a(\beta)^{-(L-\ell)}$, respectively, where $a(\beta) > 1$ and $Q(\beta)$ are $O(1)$ constants dependent only on β. We note that the constant $a(\beta)$ can be taken the same both for A and B because of translation invariance of the system. Finally, we reach a simple expression,

$$\boxed{S_2(\ell) = \ell \ln a(\beta) - \ln\left(1 + a(\beta)^{-L+2\ell}\right) + \ln K(\beta)}, \tag{2.11}$$

where $K(\beta) := R(\beta)/Q(\beta)$. This is the first main result of this thesis. In a similar manner, general nREE ($n > 2$) can be simplified and one can reach similar formulas. For example, the 3REE is

$$S_3(\ell) = \ell\frac{\ln b}{2} - \frac{1}{2}\ln\left(1 + K_1'\frac{b^\ell}{a(\beta)^L} + b^{-L+2\ell}\right) + \ln K_2', \tag{2.12}$$

where b, K_1' and K_2' are $O(1)$ constants that depend only on β and $a(\beta)$ is common in the 2REE (Eq (2.11)). We note that the term N in Eq. (2.8) is neglected in the above expression because it is estimated to be small compared with the other terms.

A lot of implications can be observed in Eq. (2.11). It tells that the whole 2REE curve is determined by only two parameters, $a(\beta)$ and $K(\beta)$. The first term of Eq. (2.11) denotes the volume law of entanglement for $\ell \leq L/2$, and its slope $\ln a(\beta)$ is a density of the 2REE in the thermodynamic limit $L \to \infty$. The third term $\ln K$ is an offset of the volume law. The second term, most importantly, describes the deviation from the volume law. As ℓ approaches $L/2$, this quantum correction to the volume law becomes large and eventually gets to $\ln(1+1) = \ln 2$ at $\ell = L/2$, *irrespective* of the inverse temperature β and the Hamiltonian. This is a unique feature of the 2REE as we do not observe such universal behaviors in the nREEs for $n \geq 3$. We also note that the formula (2.11) is universal among spin systems, bosonic systems, and fermion systems because we have only used the thermodynamic properties of the system in the derivation[3].

Lastly, we remark on the validity of the approximations (Eq. (2.9) and $Z_A(2\beta)/Z_A(\beta)^2 \approx Q(\beta)a(\beta)^{-\ell}$, $Z_B(2\beta)/Z_B(\beta)^2 \approx Q(\beta)a(\beta)^{-L+\ell}$) and the effect of subleading corrections of them to the formula (2.11). Those approximations are based on the extensiveness of the (sub)system, so they must be independent of whether the system is critical, integrable, and so on. Thus they are thought to be valid when $\ell, L-\ell$ is much larger than trivial length scales of the system such as the range of the interaction. In addition, ℓ and $L-\ell$ should be large enough so that there are a large number of energy eigenstates in the energy spectrum of the subsystems around the energy expectation values ($E_{A,B}(\beta)$). We denote the length scale where both conditions above are satisfied as ℓ_{ext}. We stress that the correlation length of the system does not play an important role for the extensiveness of the system. As for the subleading corrections, we can write

$$Z(\beta) = c(\beta)(1 + f_{\beta,L}(\ell))Z_A(\beta)Z_B(\beta), \quad \mathrm{tr}_A(\mathrm{tr}_B\, e^{-\beta H})^2 = c'(\beta)(1 + g_{\beta,L}(\ell))Z_A(2\beta)Z_B(\beta)^2,$$
$$Z_A(2\beta)/Z_A(\beta)^2 = Q(\beta)(1 + h_{\beta,L}(\ell))a(\beta)^{-\ell},$$

where $c(\beta), c'(\beta)$ are $O(1)$ constants independent of ℓ, and f, g, h are subleading corrections of the approximations which vanish, or become $o(1)$, for $\ell, L-\ell \gg \ell_{\text{ext}}$. By taking

[3] For bosonic systems one should be careful about a case of $\beta = 0$ and $\beta = \infty$ where there will be some divergence in physical quantities. The formula is still valid as long as $0 < \beta < \infty$ for bosonic systems.

into account these subleading corrections, we reach

$$\begin{aligned} S_2' &= \ell \ln a - \ln\left(1 + \frac{1+g_{\beta,L}(L-\ell)}{1+g_{\beta,L}(\ell)} \frac{1+h_{\beta,L}(L-\ell)}{1+h_{\beta,L}(\ell)} a^{-(L-2\ell)}\right) + \ln K(\beta) \\ &\quad + \ln\left(\frac{(1+g_{\beta,L}(\ell))(1+h_{\beta,L}(\ell))}{(1+f_{\beta,L}(\ell))^2}\right). \end{aligned}$$

When L is fixed and large enough, there is a region where $\ell, L-\ell \gg \ell_{\rm ext}$ is satisfied (note that $\ell_{\rm ext}$ does not depend on L). In that region, the subleading corrections f, g, h get sufficiently small ($o(1)$), so that our formula (2.11) holds[4].

2.2.3 Comments on relation to the area law ($\beta = \infty$) and the random state ($\beta = 0$)

We comment on the relation between Eq. (2.11) and the celebrated area-law of entanglement for the ground state [17, 18]. When $\beta = \infty$ the cTPQ state reduces to the ground state $|GS\rangle$, so the area law of entanglement will appear; in our setup, $S_n(\ell) = \text{const}$. Indeed, the derivation of the volume-law formula (2.11) fails at the approximation $\frac{Z_A(2\beta)}{Z_A(\beta)^2} \propto a(\beta)^{-\ell}$ because $Z_A(\beta = \infty) = 1$. At $\beta = \infty$, the term $\ln R(\beta)$ in Eq. (2.10) which comes from the boundary of two subsystems becomes important and responsible for the area law (with a possible logarithmic correction).

We also take a quick look at the case of infinite temperature $\beta = 0$. When $\beta = 0$, the cTPQ state (2.1) reduces to a random state and we can obtain a simple equation for general n:

$$S_n = \ell \ln d - \frac{1}{n-1} \ln\left[\sum_{k=1}^{n} N(n,k) \left(\frac{\lambda^\ell}{\lambda^{L-\ell}}\right)^{k-1}\right], \tag{2.13}$$

where the local dimension of the Hilbert space is λ (for qubit systems $\lambda = 2$), and $N(n,k) = \frac{1}{n}\binom{n}{k}\binom{n}{k-1}$ is known as the Narayana numbers. When $n = 2$, this expression reproduces the previous results of the 2REE of the random state in Refs. [75, 76],

$$S_2 = -\ln\left(\frac{\lambda^\ell + \lambda^{L-\ell}}{\lambda^L + 1}\right) = \ell \ln \lambda - \ln\left(1 + \lambda^{L-2\ell}\right), \tag{2.14}$$

where we have ignored 1 in the denominator.

2.3 Numerical check of the universal functional form (2.11) for the cTPQ states

In order to confirm the validity of the approximations and clarify the advantages of our formula (2.11), we present numerical simulations of the 2REE curve of the cTPQ states

[4] The second term is $\ln\left(1 + (1+o(1))a^{-(L-2\ell)}\right) = \ln\left(1 + a^{-(L-2\ell)}\right) + o(1)$ and the last term is $\ln(1+o(1)) = o(1)$.

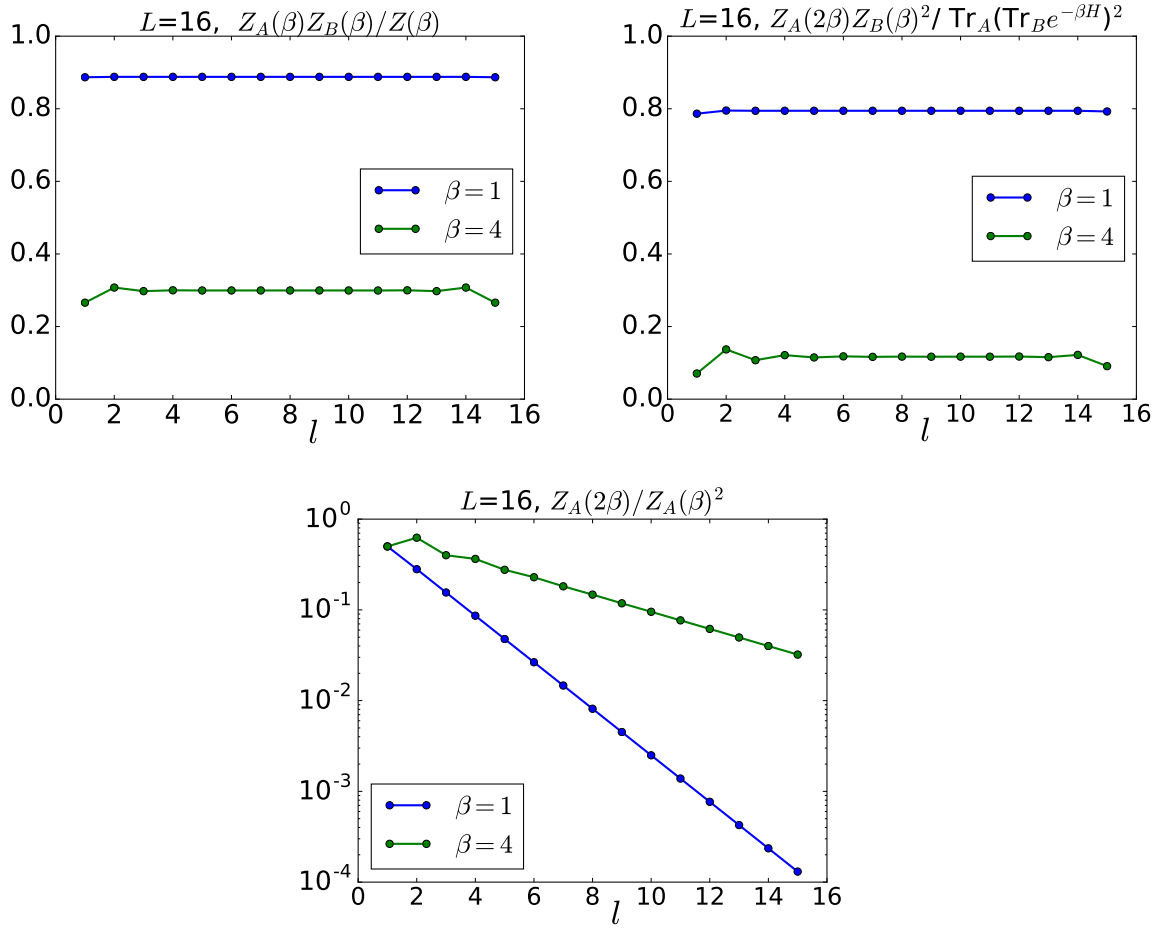

Figure 2.2: Numerical results of $Z_A(\beta)Z_B(\beta)/Z(\beta)$ (top left), $Z_A(2\beta)Z_B^2(\beta)/\,\mathrm{tr}_A\left(\mathrm{tr}_B\, e^{-\beta H}\right)^2$ (top right), and $Z_A(2\beta)/Z_A(\beta)^2$ (bottom) in the XX chain (2.15) of $L = 16$ as a function of the subsystem size ℓ.

for the $S = 1/2$ XX chain under a periodic boundary condition,

$$H = \sum_{i=1}^{L} \left(S_i^x S_{i+1}^x + S_i^y S_{i+1}^y \right), \tag{2.15}$$

where S_i^x, S_i^y are the spin $S = 1/2$ operators on site i. This system is mapped to the free fermion system by the Jordan-Wigner transformation [77], and the quantities $\mathrm{tr}_A(\mathrm{tr}_B\, e^{-\beta H})^2$ and $\mathrm{tr}_B(\mathrm{tr}_A\, e^{-\beta H})^2$ can be efficiently calculated in a large system ($L \sim 100$) by the correlation functions of the system [78].

First, we check the validity of approximations Eq. (2.9) and $Z_A(2\beta)/Z_A(\beta)^2 \propto a(\beta)^{-\ell}$ used in the derivation of the Eq. (2.11). Figure 2.2 shows the numerical results of $Z_A(\beta)Z_B(\beta)/Z(\beta)$, $Z_A(2\beta)Z_B(\beta)^2/\,\mathrm{tr}_A\left(\mathrm{tr}_B\, e^{-\beta H}\right)^2$, and $Z_A(2\beta)/Z_A(\beta)^2$ in the XX chain (2.15) of $L = 16$ at inverse temperature $\beta = 1$ and 4. As clearly seen from the figures, $Z_A(\beta)Z_B(\beta)/Z(\beta)$ and $Z_A(2\beta)Z_B(\beta)^2/\,\mathrm{tr}_A\left(\mathrm{tr}_B\, e^{-\beta H}\right)^2$ do not depend on ℓ for $2 \lesssim \ell \lesssim L - 2$. Also $Z_A(2\beta)/Z_A(\beta)^2 \propto \exp(-\ell)$ holds well down to $\ell = 3$.

Next, we numerically calculate the 2REE of the cTPQ states at inverse temperatures

$\beta = 2$ and $\beta = 4$ by directly evaluating Eq. (2.7). In top panels of Fig. 2.3, we present the numerical data of the 2REE and the fits of them by our formula (2.11)[5]. For all system sizes L and subsystem sizes ℓ, the fitting works quite well. In addition, we compare several estimations of the density of the 2REE from the numerical data in order to illustrate the advantage of our formula. We extract the density of the 2REE from the numerical data in three ways: $\ln a$ from the fits by our formula, the density of the 2REE for half of the system, $S_2(L/2)/(L/2)$, and the average slope of the curve between $\ell = 1$ and $\ell = 5$, $(S_2(5) - S_2(1))/4$. From the bottom panels of Fig. 2.3, it is clear that $\ln a$ does not contain any systematic error and converges rapidly as large L compared with the other two estimates, which manifests one of the practical advantages of our formula (2.11).

[5] The fitting is performed for the data of $\{S_2(\ell)\}_{\ell=1}^{\ell=L-1}$ by setting a and K in Eq. (2.11) as fitting parameters, through the least squares method implemented in the numerical package `scipy.optimize.leastsq`.

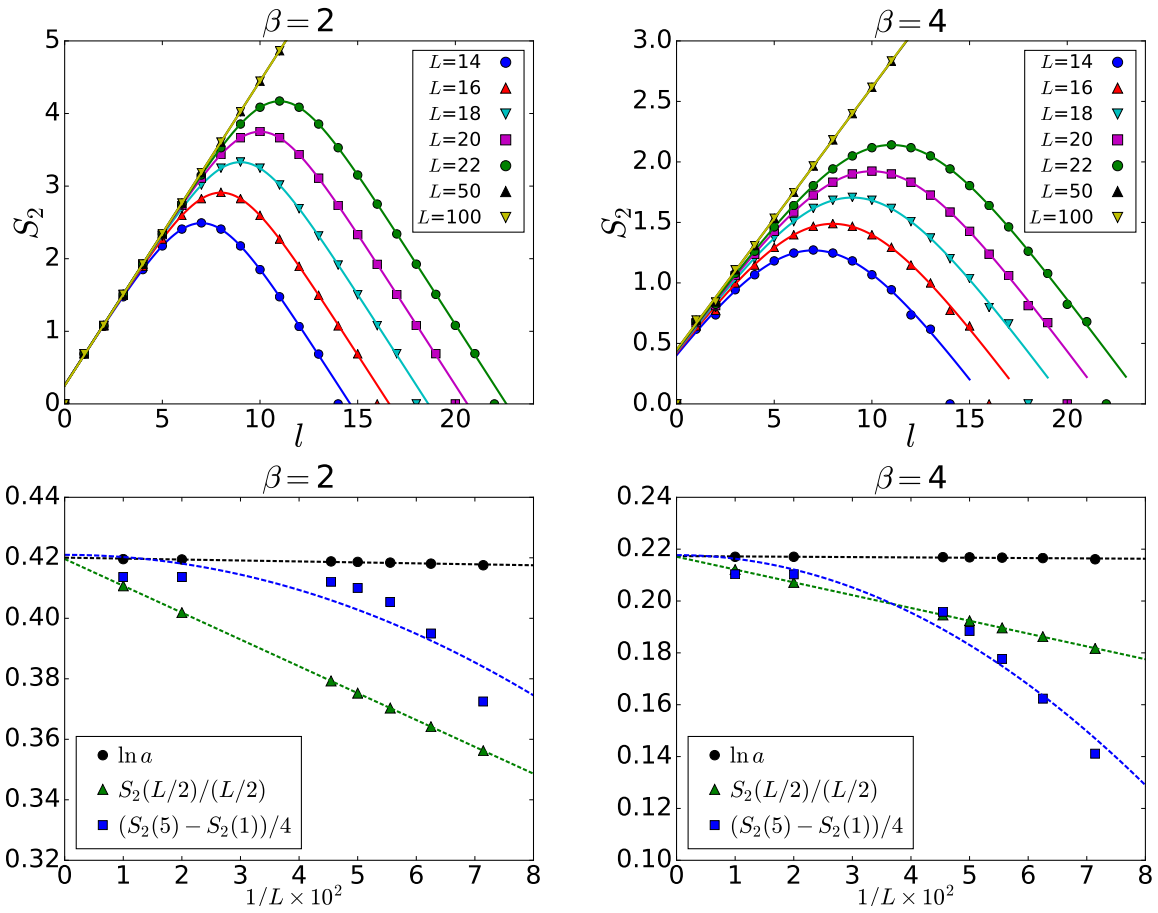

Figure 2.3: The second Rényi entanglement entropy of the cTPQ states. (top) The dots are the 2REE of the cTPQ states of the XX chain (2.15) at inverse temperature $\beta = 2$ (left) $\beta = 4$ (right) calculated by Eq. (2.7) for various system sizes L. The lines are the fits by Eq. (2.11) for the numerical data. (bottom) Comparison among $\ln a$, $S_2(L/2)/(L/2)$, and $(S_2(5) - S_2(1))/4$. The dashed lines are extrapolations to $L \to \infty$ by $1/L$ scaling for $\ln a$ and $S_2(L/2)/(L/2)$ and by $1/L^2$ scaling for $(S_2(5) - S_2(1))/4$. All three data coincide at the thermodynamic limit $L \to \infty$ but the extent of the convergence in L is different.

2.4 Conjecture for applicability of the formula to general pure states

We have derived the functional form of the volume law of the 2REE (Eq. (2.11)) and how well it describes the numerical data of the cTPQ states. However, there are many kinds of thermal pure states other than the cTPQ states; the cTPQ state is just a canonical and analytically-tractable example of thermal pure states. In this section, we discuss the applicability of the formula to general pure states.

For a given pure state $|\psi\rangle = \sum_i c_i |i\rangle$, where $\{|i\rangle\}_i$ is some complete basis of the system, one obtains by definition

$$S_2 = -\ln\left(\mathrm{tr}_A\, \rho_A^2\right) = -\ln\left(\mathrm{tr}_A\left(\sum_{i,j,k,l} c_i c_j^* c_k c_l^*\, \mathrm{tr}_B\left(|i\rangle\langle j|\right)\mathrm{tr}_B\left(|k\rangle\langle l|\right)\right)\right). \tag{2.16}$$

We can decompose the summation into a contribution from the "diagonal ensembles" and that from others as

$$S_2 = -\ln\left[\mathrm{tr}_A\left(\mathrm{tr}_B\left(\hat{\rho}_{\mathrm{dia}}\right)^2\right) + \mathrm{tr}_B\left(\mathrm{tr}_A\left(\hat{\rho}_{\mathrm{dia}}\right)^2\right) + I_{\mathrm{off}}\right], \tag{2.17}$$

where the diagonal ensemble (dependent on a choice of the basis) is defined as

$$\hat{\rho}_{\mathrm{dia}} := \sum_i |c_i|^2 |i\rangle\langle i|, \tag{2.18}$$

and the off-diagonal contribution I_{off} is

$$I_{\mathrm{off}} := \mathrm{tr}_A\left(\sum_{i,j,k,l}{}' c_i c_j^* c_k c_l^*\, \mathrm{tr}_B\left(|i\rangle\langle j|\right)\mathrm{tr}_B\left(|k\rangle\langle l|\right)\right). \tag{2.19}$$

Here, the summation $\sum'$ runs all (i,j,k,l) without those satisfying $(i,k) = (j,l)$ or $(i,k) = (l,j)$.

From Eq. (2.17), we can see that our formula (2.11) will apply to the 2REE of $|\psi\rangle$ if

(1) I_{off} is absent or negligible, and

(2) The 2REE of ρ_{dia} is extensive with a constant density, i.e.,

$$\mathrm{tr}_A\left(\mathrm{tr}_B\left(\hat{\rho}_{\mathrm{dia}}\right)^2\right) \approx c\cdot a^{-\ell},\ \mathrm{tr}_B\left(\mathrm{tr}_A\left(\hat{\rho}_{\mathrm{dia}}\right)^2\right) \approx c\cdot a^{-(L-\ell)}, \tag{2.20}$$

where a and c are constants *independent* of ℓ.

This is because by putting the above equations into Eq. (2.17) and neglecting I_{off} it follows that

$$S_2(\ell) = -\ln\left(a^{-\ell} + a^{-(L-\ell)}\right) - \ln c = \ell \ln a - \ln(1 + a^{-(L-2\ell)}) - \ln c, \tag{2.21}$$

which is exactly the same form of our formula (2.11).

We have several comments on these two conditions.

- First, we think that the negligibility of the off-diagonal contribution I_{off} is not so special but rather common in general thermal pure states, because the coefficients $\{c_i\}_i$ of typical pure states are expected to be uncorrelated in general [39]. Say that $\{c_i\}_i$ are uncorrelated random numbers, then the off-diagonal term I_{off} will die out for large systems without taking average of the random numbers due to the central limit theorem. This is what happens for the cTPQ states. In general thermal pure state the coefficients are not random numbers, but we expect that the uncorrelated nature of them results in the negligibility of I_{off}. We call pure states whose coefficients $\{c_i\}_i$ are uncorrelated as "**scrambled**" states, although the definition of them depends on the basis in which we expand the states. In most cases we take the basis as a local basis (such as $\{|\uparrow\uparrow\uparrow\cdots\rangle, |\uparrow\uparrow\downarrow\cdots\rangle, \ldots\}$ in $S = 1/2$ spin systems), or as energy eigenstates $\{|E_i\rangle\}_i$ of the system.

- Second, the extensiveness of 2REE for the diagonal ensemble is not guaranteed in general and it has to be checked for each specific case. In the case of the cTPQ states, the diagonal ensemble after the random average is the Gibbs state $\rho_{\text{dia,cTPQ}} = e^{-\beta H}/Z(\beta)$ and the extensiveness is apparent (note that the basis dependence disappears in this case because of the random average). If one considers stationary states after quantum quench as we will do in Chapter 3, it is useful to take energy eigenstates of a system as a basis to define the diagonal ensemble. Indeed, the diagonal ensemble in the energy eigenstate basis has been studied by many authors in connection with thermodynamic entropy, and the vN-EE of it (called diagonal entropy) is known to behave consistently with the thermodynamic laws [79, 80]. Therefore it is natural to expect that the 2REE of the diagonal ensemble in the energy eigenstate basis exhibits the thermodynamic behavior, or the extensiveness. On the other hand, for energy eigenstates in non-integrable systems which are also believed to be thermal, the extensiveness of the 2REE of ρ_{dia} is weakly broken [68] and the applicability of the formula (2.11) becomes approximate (see Chapter 4).

- Third, strictly speaking, the conditions (1)(2) are only sufficient for the formula to hold. The uncorrelated or scrambled nature of the coefficients $\{c_i\}_i$, however, is expected in any typical (thermal) pure state [39], so we exclude a possibility that the formula (2.11) will hold without the conditions (1)(2) throughout all discussions in this thesis.

Based on the above considerations, we conjecture the following statement:

Conjecture. *The equation* (2.11)*, named as the volume-law scaling formula, applies to the second Rényi entanglement entropy of general thermal pure states and general scrambled states as a fitting function with the fitting parameters* $a(\beta)$ *and* $K(\beta)$*.*

In the following chapters, we numerically examined this conjecture by taking (a) stationary states after quantum quench (Chapter 3) and (b) energy eigenstates of general Hamiltonians (Chapter 4) as examples.

Chapter 3

Application of the volume-law scaling formula to stationary states after quantum quench

In this chapter, as a nontrivial test of the validity of our formula in general thermal pure states, we numerically investigate stationary pure states after quantum quench. Such stationary states are considered as thermal if a system is non-integrable but *athermal* if integrable. Our numerical results by exact diagonalization in spin chain models show that the formula (2.11) applies to the stationary states after quantum quench in non-integrable model *and* in interacting-integrable models. We ascribe the reason for this somewhat unexpected result to the scrambling nature of the wave function invoked by time-evolution after quantum quench. To confirm the above argument further, we also present a numerical result of the quench in quadratic-integrable models where there is no scrambling after time-evolution. Finally, we show that the recent experimental results of the 2REE can actually be fitted by our formula.

3.1 Quantum quench in closed quantum systems and thermalization

Quantum quench means a sudden change of parameter(s) in a quantum system and has been featured in recent studies of condensed matter physics as well as high-energy physics [12, 15, 16, 42–48, 58, 81–89]. It is one of the simplest protocols to make systems nonequilibrium and study the nature of such situations. In studies of quantum quench, an initial state is typically prepared as the ground state of pre-quench Hamiltonian, and then a parameter of the system (Hamiltonian) is changed in time. Since the initial state is not in general the eigenstate of the post-quench Hamiltonian, there occurs non-trivial dynamics in the system, and one can study the dynamics itself and/or its long-time limit by the quantum quench protocol.

One of the most fundamental questions that can be addressed by quantum quench is the problem of thermalization in closed quantum systems, which was briefly mentioned in the last part of section 1.2. Let us denote the time-dependent Hamiltonian

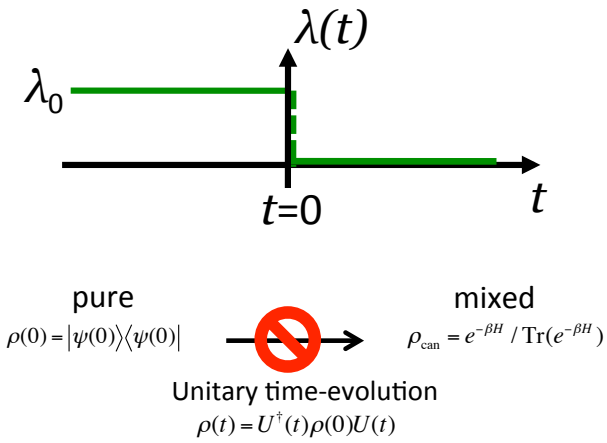

Figure 3.1: Schematic picture of quantum quench. (top) A parameter $\lambda(t)$ in a system is abruptly changed at time $t = 0$ and it will invoke non-trivial dynamics in the system. (bottom) Since the unitary time-evolution $U(t)$ keeps the pure state $\rho(0)$ being pure, it cannot relax into the mixed-state thermal ensembles.

as $H(t)$ and an initial pure state as $|\psi(0)\rangle$ in quantum quench. Since time-evolution in closed quantum systems is described by the unitary operator $U(t) = \mathcal{T} e^{-i\int_0^t ds H(s)}$, where $\mathcal{T}$ is the time-ordered product, the purity of the initial state is preserved: $\mathrm{tr}\,\rho(t)^2 = \mathrm{tr}\left(U^\dagger(t)\rho(0)U(t)\right)^2 = \mathrm{tr}\,\rho(0)^2 = 1$. Hence the initial state remains pure under time-evolution and cannot relax into the mixed-state thermal ensembles (see Fig. 3.1). In this case, one should consider a *local* thermalization of the system, which is defined as

$$\exists \rho_{\mathrm{Gibbs}}(\beta), \quad \lim_{T\to\infty} \frac{1}{T}\int_0^T ds\, \langle\psi(s)|\hat{A}|\psi(s)\rangle = \mathrm{tr}\left(\rho_{\mathrm{Gibbs}}(\beta)\hat{A}\right) \quad \text{for all local } \hat{A}. \tag{3.1}$$

We note that the time average is introduced in the left hand side to avoid recurrence due to the finite size effect and that the exact equality holds only in the thermodynamic limit. Equation (3.1) implies that a stationary state after quench in a closed quantum system can be considered as a thermal pure state if thermalization occurs and the temporal fluctuation of $\langle\psi(t)|A|\psi(t)\rangle$ is small.

Thermalization in terms of (3.1) is widely believed to happen in general interacting systems (for a review, see Refs. [44, 47]). Intuitive understanding of the thermalization can be made by the typicality introduced in section 1.2. Most of the pure states in the Hilbert space look thermal and athermal states (including the initial state of quantum quench) are very rare, so the dynamics in the Hilbert space from the initial state will easily bring it to some thermal state. Furthermore, there is a more quantitive and attractive augment for the cause of the thermalization named the Eigenstate Thermalization hypothesis (ETH) [90–92], which we will discuss in detail in section 4.1. A general proof of the thermalization in closed quantum systems, nevertheless, has been still lacking.

On the other hand, there is an important exception for the thermalization in closed quantum systems. In the so-called integrable systems, it is believed that no thermalization occurs even in the sense of Eq. (3.1). Here, we call quantum many-body systems which

are exactly solved by the Bethe ansatz and have infinitely many conserved quantities as integrable systems[1] [94]. The reason for the absence of thermalization in integrable systems is naively understood by the fact that the infinitely many conserved quantities restrict the dynamics of the state in the Hilbert space so that it cannot reach "typical" thermal states. Nevertheless, one can construct another statistical ensemble describing stationary states after quantum quench in integrable systems: Generalized Gibbs ensemble (GGE) [82]. GGE is defined through additional conserved quantities other than the Hamiltonian (energy),

$$\rho_{\mathrm{GGE}}^{\beta,\{\lambda_i\}} = \frac{1}{Z_{\mathrm{GGE}}} \exp\left(-\beta H - \sum_i \lambda_i Q_i\right), \tag{3.2}$$

where Q_i are conserved quantities[2] in a system, $\{\lambda_i\}$ are Lagrange multipliers and Z_{GGE} is a normalization constant. Relaxation after quantum quench in integrable systems is described by replacing the Gibbs state $\rho_{\mathrm{Gibbs}}(\beta)$ in Eq. (3.1) with the GGE $\rho_{\mathrm{GGE}}^{\beta,\{\lambda_i\}}$. A number of papers confirmed the validity of the GGE in many kinds of integrable models [44, 81–83, 86, 95, 96], and the relaxation to the GGE was observed in experiments [42, 45].

In the following sections, we investigate the 2REE of stationary states after quantum quench both for integrable and non-integrable models.

3.2 Numerical results

We consider the $S = 1/2$ Heisenberg model up to next-nearest neighbor interactions under periodic boundary condition,

$$H = \sum_{i=1}^{L} \left(\boldsymbol{S}_i \cdot \boldsymbol{S}_{i+1} + J_2 \boldsymbol{S}_i \cdot \boldsymbol{S}_{i+2}\right), \tag{3.3}$$

where $\boldsymbol{S}_i = (S_i^x, S_i^y, S_i^z)$ is the $S = 1/2$ spin operators on site i. This model can be thought as a prototype of quantum many-body systems and the quantum quench in this model has been explored by a lot of papers [82, 83, 95, 97–99]. This model is known to be non-integrable for $J_2 \neq 0$ and integrable for $J_2 = 0$. In numerical calculation, we employ[3] $J_2 = 0.5$ ($J_2 = 0$) as a non-integrable (integrable) case. The initial state of the quench is taken to be the Néel state $|\text{Néel}\rangle := |\uparrow\downarrow\uparrow\downarrow\uparrow\downarrow \ldots\rangle$ and we compute the dynamics after the quench, $|\psi(t)\rangle = e^{-iHt}|\text{Néel}\rangle$, by exact diagonalization. We take a time step of evolution as $dt = 0.1$ and calculate the dynamics of 2REE curve $S_2(t, \ell)$ up to $t \leq T = 300$.

3.2.1 Non-integrable case

The numerical results for the non-integrable model ($J_2 = 0.5$) with the system size $L = 16$ are presented in the top left panel of Fig. 3.2 (interested readers can find animations of the

[1] We include quadratic models such as free particle systems in the definition of integrable models. We note that the complete definition of integrability and integrable systems is still under active discussion [93].

[2] Operators which commute with the Hamiltonian: $[Q_i, H] = 0$.

[3] The model with $J_2 = 0.5$ is known as Majumdar-Ghosh model where the ground state is exactly obtained [100]. However, general excited states are not analytically calculable so we call the model as non-integrable.

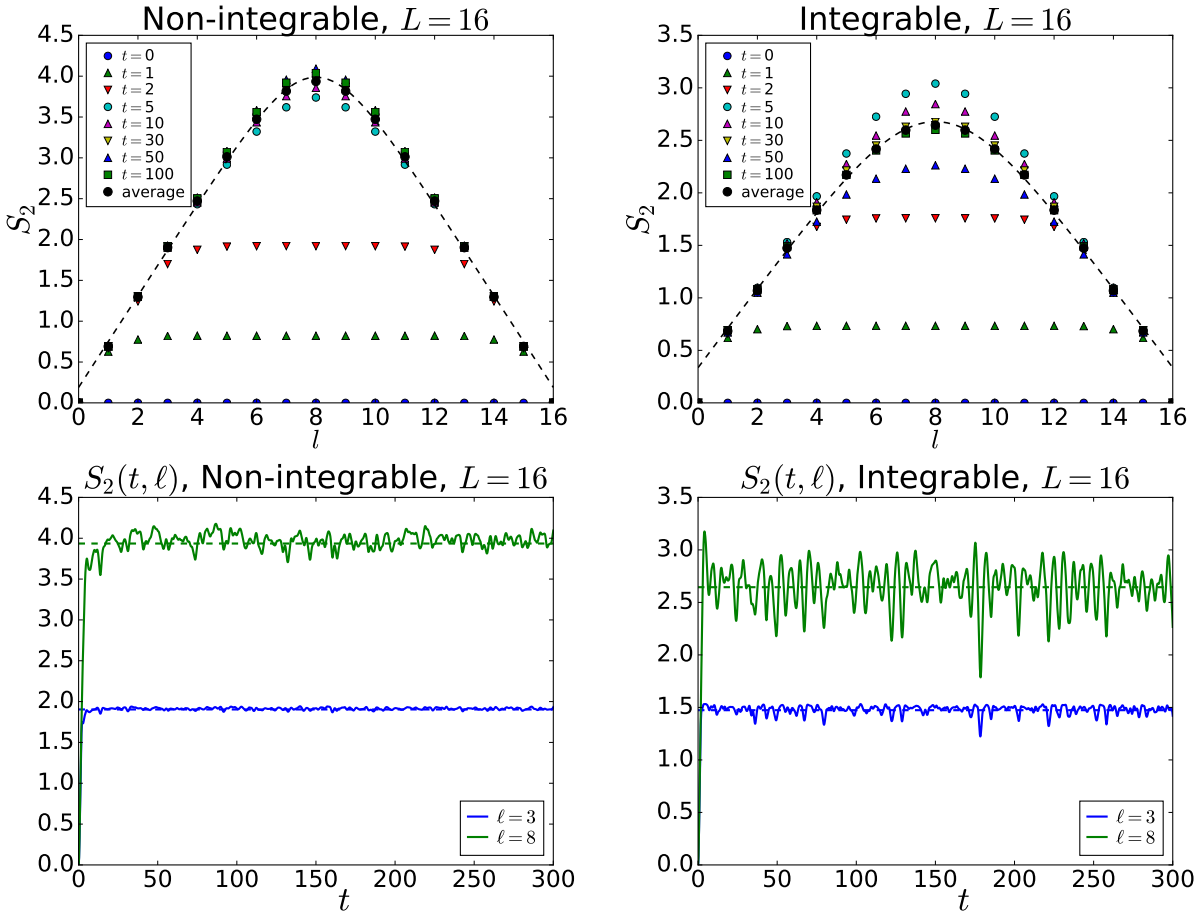

Figure 3.2: Dynamics of the second REE curve $S_2(t,\ell)$ after quantum quench. (top panels) Time-evolution of the 2REE after quantum quench from the Néel state. The dashed line is the fit by Eq. (2.11) for the time average of $S_2(t,\ell)$. The left panel is for the non-integrable Hamiltonian (Eq. (3.3) with $J_2=0.5$ and $L=16$) and the right one is for the integrable Hamiltonian ($J_2=0, L=16$). (bottom panels) The dynamics of the 2REE at $\ell=3$ and $\ell=L/2=8$. The dashed lines indicate the values of the time average.

dynamics in ancillary files of arXiv:1703.02993v1). Initially at $t = 0$, the 2REE curve is flat because the initial state is the Néel state which has no entanglement at all. After the quench ($t > 0$) the thermalization starts to take place and the volume law of entanglement appears. Since the numerical data oscillate in time as long as $t = T = 300$ due to the finite size effect (as seen in the bottom left panel of Fig. 3.2), we calculate the long-time average of the 2REE curve $S_2(t, \ell)$,

$$\bar{S}_2(\ell) := \frac{1}{T}\int_0^T dt S_2(t, \ell), \tag{3.4}$$

as an estimation of the long-time limit $\lim_{t\to\infty} S_2(t, \ell)$. Clearly, one can tell from the top left panel of Fig. 3.2 that the time average of $\bar{S}_2(\ell)$ (black circles) is well fitted by our formula (2.11) (dashed line). The figure illustrates the validity of our formula for stationary states after quantum quench in non-integrable systems.

3.2.2 Integrable case

In the right panels of Fig. 3.2 the numerical data of the quench for the integrable model ($J_2 = 0$) are shown. The qualitative dynamics is the same as in the integrable case; the 2REE curve $S_2(\ell, t)$ starts from the flat line and eventually exhibits the volume law. Somewhat surprisingly, the fitting to the long-time average $\bar{S}_2(\ell)$ by our formula (2.11) also works well in this integrable model. As explained in the previous section, there is no thermalization in integrable systems so that other local observables, such as staggered magnetization, are not explained by the cTPQ states or mixed-state thermal ensembles [82, 83, 95]. In this sense, the applicability of the formula (2.11) which is derived for thermal pure states is rather a special feature of the 2REE, and we will discuss the reason in the next section.

In addition, we find that the temporal fluctuation in the integrable case is larger than that in the non-integrable case as implied in the bottom panels of Fig. 3.2. This is because the infinitely many conserved quantities in the system make the number of effective degrees of freedom small. As presented in Fig. 3.3, we observe that the fluctuation possibly decays algebraically with the system size L for the integrable case, whereas it decays exponentially in the non-integrable case. This is in contrast to Ref. [101] where the fluctuation of local observables in the same integrable model as ours exhibits the exponential decay with the system size. We think the difference is due to either a genuine characteristic of the non-local nature of the 2REE or simply the finite size effect of our numerical calculation. We note that $S_2(L/2)/L$ has a support as large as half of the system so that the finite size effect would be strong compared with local observables.

3.3 Discussion on applicability of the formula by time average

The reason why the result of the integrable model (Eq. (3.3) with $J_2 = 0$) is well fitted by our formula can be explained by the uncorrelated or scrambled nature of the wave function after time-evolution introduced in section 2.4.

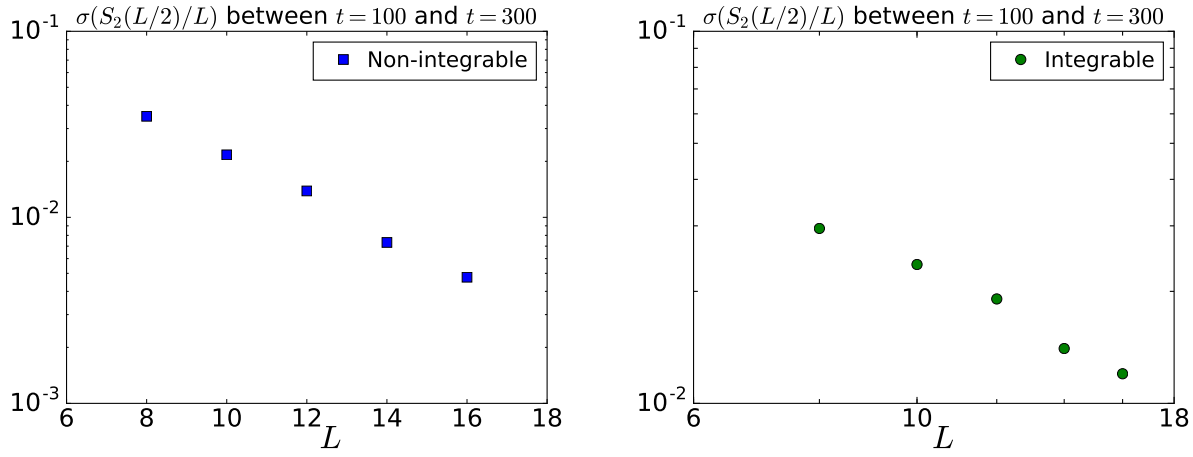

Figure 3.3: Temporal fluctuations of a density of the 2REE at the center of the system, $S_2(L/2)/L$. We calculate the standard deviation of the $\{S_2(t, L/2)/L\}_{t=100}^{t=300}$, where the time t is discretized in $dt = 0.1$. The left panel is the result for the non-integrable system (Eq. (3.3) with $J_2 = 0.5$) in a semilog scale and the right panel is for the integrable system ($J_2 = 0$) in a log-log scale. One can see that the fluctuation in time decays exponentially with the system size L in the non-integrable model but algebraically in the integrable model.

First, let us consider a slightly different time average of the 2REE from what is considered in the numerical calculation (we omit ℓ in this section for brevity),

$$\overline{S_2}^{\text{time}'} = -\ln\left(\lim_{T\to\infty}\frac{1}{T}\int_0^T dt\,\mathrm{tr}_A(\rho_A(t))^2\right). \tag{3.5}$$

If one assumes that $S_2(t)$ reaches a stationary value at $t \to \infty$ with a small temporal fluctuation (which is the case for large L (Fig. 3.3)), two time-averages coincide with each other.

Next let us take the energy eigenstates $\{|n\rangle_E\}_n$ as a basis and expand the initial state of the quench as $|\psi(0)\rangle = \sum_n c_n |n\rangle_E$. Thanks to the choice of the basis it is easy to write down the time-evolution after the quench, and the density matrix for $t > 0$ is

$$\rho(t) = |\psi(t)\rangle\langle\psi(t)| = \sum_{n,m} c_n c_m^* e^{-i(E_n-E_m)t}|n\rangle_E\langle m|_E. \tag{3.6}$$

By taking partial trace of the subsystem B one obtains the reduced density matrix on A as

$$\rho_A(t) = \mathrm{tr}_B\,\rho(t) = \sum_{n,m} c_n c_m^* e^{-i(E_n-E_m)t}\rho_A(n;m), \tag{3.7}$$

where $\rho_A(n;m) := \mathrm{tr}_B\,(|n\rangle_E\langle m|_E)$. Thus the time-averaged REE is written as

$$\overline{S_2}^{\text{time}'} = -\ln\left(\sum_{n,m,k,l}{}' c_n c_m^* c_k c_l^*\ \mathrm{tr}_A\left(\rho_A(n;m)\rho_A(k;l)\right)\right), \tag{3.8}$$

where the summation is taken over the indices satisfying $E_n - E_m + E_k - E_l = 0$. In general interacting systems, regardless of integrable or non-integrable, it is quite rare to satisfy this condition except for the trivial solutions of it, $(n = m;\ k = l)$ or $(n = l;\ k = m)$ [101,102]. Hence we assume that the dominant contribution in Eq. (3.8) comes from those trivial combinations of the indices, we reach a simple expression:

$$\overline{S_2}^{\text{time}'} = -\ln\left[\mathrm{tr}_A(\mathrm{tr}_B\,\rho_{\text{diag},E})^2 + \mathrm{tr}_B(\mathrm{tr}_A\,\rho_{\text{diag},E})^2\right], \tag{3.9}$$

where $\rho_{\text{diag},E} = \sum_n |c_n|^2 \,|n\rangle_E \,\langle n|_E$ is the diagonal ensemble in the energy eigenstate basis.

Equation (3.9) implies that the time average of the 2REE does not contain the off-diagonal term I_{off} in Eq. (2.17) due to the "dephasing" induced by interactions of the system during time-evolution. Moreover, the diagonal ensemble in the energy eigenstates basis is expected to be extensive[4] as we discussed in section 2.4. Therefore, the time-averaged 2REE in interacting systems, regardless of integrable or non-integrable, obeys our formula (2.11) because two conditions in section 2.4 are reasonably satisfied.

3.4 Further results for quadratic-integrable models: where there is no scrambling

In order to confirm the above scenario, we examine quantum quench in other integrable models where there is no scrambling at all even after a long time. The important point of the discussion in the previous section is that the condition $E_n - E_m + E_k - E_l = 0$ is satisfied only for trivial combinations of indices, $(n = m;\ k = l)$ and $(n = l;\ k = m)$. This is the case for interacting-integrable models[5], but not the case for "quadratic-integrable models" which are equivalent to some quadratic (or free-particle) Hamiltonian. The notion of one-particle spectrum holds well in such quadratic models and therefore the condition $E_n - E_m + E_k - E_l = 0$ is satisfied for a lot of non-trivial sets of indices[6] (similar discussion is found in Refs. [101,105]). In the following, we study two specific examples of quadratic-integrable models.

3.4.1 $S = 1/2$ XX chain

A first example of quadratic-integrable models is the $S = 1/2$ XX chain (2.15). Again we numerically calculate the quantum quench from the Néel state[7], $|\text{Néel}\rangle = |\uparrow\downarrow\uparrow\downarrow\uparrow\downarrow \ldots\rangle$. The results are shown in Fig. 3.4. Apparently the fit by our formula (2.11) (black dashed line in the left panel) is not well for the time-averaged value of $S_2(t, \ell)$ from $t = 0$ to $t = 300$. This is consistent with the discussions above. Moreover, the temporal fluctuation is found

[4] We consider the extensiveness, which is one of the most fundamental properties of quantum many-body system, is not affected by the integrability of a system.

[5] We denote integrable models which are not equivalent to any quadratic model as "interacting-integrable models".

[6] We note that some exceptional interacting-integrable systems which have larger symmetries compared with the usual Bethe-ansatz solvable models, such as the Haldane-Shastry model [103,104], may also fall into the same class as quadratic-integrable models because their energy spectra are quite simple.

[7] Although the system is completely free, the Néel state is not an eigenstate of the system and there will happen non-trivial dynamics after the quench.

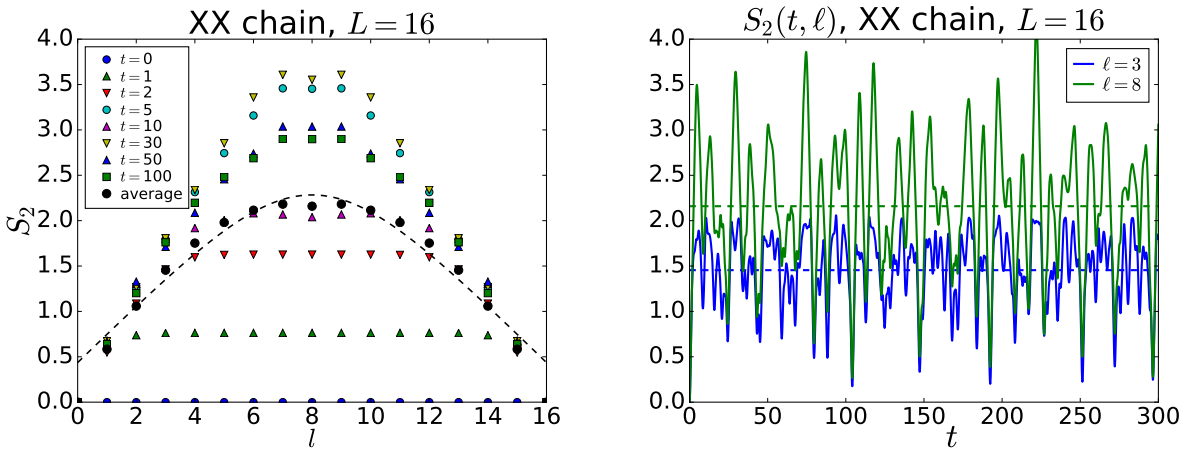

Figure 3.4: The dynamics of $S_2(t,\ell)$ for the quantum quench from the Néel state in the XX chain (2.15). (left) ℓ-dependence at several fixed times t. The black dots are the time average of the $S_2(t,\ell)$ from $t=0$ to $t=300$. The black dashed line is the fitting of them by the formula (2.11). (right) t-dependence at fixed ℓ. Horizontal dashed lines indicate the values of the time average.

to be by far larger than that of the Heisenberg model (bottom right panel of Fig. 3.2) as seen in the right panel of Fig. 3.4.

3.4.2 Free relativistic Dirac fermions in two-dimensional space-time

We investigate a field-theoretical model as another example of quadratic-integrable models. We consider the free massless Dirac fermions in (1+1)-dimensional space-time, which reduces to the conformal field theory (CFT) in (1+1)-dimensions with the central charge $c=1$ [106]. We note that the dynamics of entanglement of (conformal) field theories after quantum quench in a *finite* system size L and at *non-zero* temperature $0<T<\infty$ has not been explored so much [58–60, 88, 107–109], although there are a number of studies for infinite system size or zero temperature [87, 89]. We also comment that in the holography (or the gauge-gravity duality [110]) it is hard to calculate the n-th Rényi entanglement entropy [111] compared with doing the entanglement entropy by the celebrated Ryu-Takayanagi formula and HRT (Hubeny-Rangamani-Takayanagi) formula [84, 112].

In Ref. [58], Ugajin and Takayanagi studied the dynamics of the entanglement entropy in (1+1)-dimensional CFT of the central charge $c=1$ consisting of the free massless Dirac fermions. The CFT lives on a circle of unit radius and the size of the subsystem A is parameterized by $\sigma\in[0,2\pi]$. They considered the dynamics of a pure state $|\psi_0\rangle=e^{-\beta H/4}|B\rangle$ on a cylinder of the length L, where $|B\rangle$ is the conformal boundary state [86, 87][8]. The time-evolution is defined as $|\psi(t)\rangle=e^{-iH_{CFT}t}|\psi_0\rangle$, where H_{CFT} is the Hamiltonian which describes the CFT. By employing the path integral formulation of the Rényi entanglement

[8] Here, the parameter β is not a temperature but a cutoff energy scale of the initial state. It is named after the fact that the stationary value of the entanglement entropy after the quench turns out to be the same as the thermal entropy of the system at inverse temperature β [87].

entropy and converting it into to a $2n$ point function of the twist operator though several conformal maps, they reached

$$S'_n(t,\sigma) = \frac{n+1}{12n}\left(2\ln\left(\frac{2\beta}{\pi a_{UV}}\right) + \ln\left(\frac{\left|\theta_1(\frac{i\sigma}{4\beta}|\frac{i\pi}{2\beta})\right|^2\left|\theta_1(\frac{\beta+it}{2\beta}|\frac{i\pi}{2\beta})\right|^2}{\eta(\frac{i\pi}{2\beta})^6\left|\theta_1(\frac{2\beta+2it+i\sigma}{4\beta}|\frac{i\pi}{2\beta})\right|\left|\theta_1(\frac{2\beta+2it-i\sigma}{4\beta}|\frac{i\pi}{2\beta})\right|}\right)\right), \tag{3.10}$$

where a_{UV} is a ultraviolet cutoff of the theory, θ_1 is a variant of the theta function, and η is the Dedekind eta function:

$$\theta_1(\nu|\tau) := i\sum_{n=-\infty}^{\infty}(-1)^n q^{(n-1)^2/2} z^{n-1/2}, \tag{3.11}$$

$$\eta(\tau) := q^{1/24}\prod_{k=1}^{\infty}(1-q^k), \tag{3.12}$$

with $q = e^{2\pi i\tau}$ and $z = e^{2\pi i\nu}$. The first term is divergent due to the cutoff a_{UV}, but has no σ dependence. Thus the volume law of entanglement will come from the second term. We call the second term as $S_n(t,\sigma)$. From the expression, one can see the symmetric and periodic properties of $S_n(t,\sigma)$,

$$S_n(t,2\pi-\sigma) = S_n(t,\sigma),\ \ S_n(t+\pi,\sigma) = S_n(t,\sigma). \tag{3.13}$$

The form of $S_n(t,\sigma)$ looks complicated, but it exhibits the volume law as shown in the numerical data for $n=2$ in the top panels of Fig. 3.5 (σ-dependence of $S_2(t,\sigma)$). We perform the fit by our formula (2.11) to those numerical data, and find that the fitting does not work well. This is again consistent with the discussion in the beginning of this section. We note that the numerical data clearly satisfies the properties (3.13) as inferred from the bottom panels of Fig. 3.5.

3.5 Application of the formula to the experimental result by Kaufman *et al.*

As a closing of this chapter, we show that our formula (2.11) is actually applicable to the experimental data.

Recently, Kaufman *et al.* experimentally measured the 2REE after quantum quench in Ref. [12]. They prepared two copies of the Bose-Hubbard model in one dimension in an optical lattice loaded with ^{87}Rb and measured the second Rényi entanglement entropy of the single system by a sophisticated many-body interference measurement of two copies [11]. They realized quantum quench in the system and observed the dynamics of the 2REE after the quench like our setup in this chapter. The initial state of the quench was prepared as a state with a single atom at all sites, which is the ground state of the Bose-Hubbard model with infinitely strong repulsive interactions. Here, we apply our formula (2.11) to their experimental results.

In Fig. 3.6, we provide a fitting of the experimental data by our formula (2.11). The data are extracted from Fig. 4A of Ref. [12] by us and all data points ($\ell = 1,\ldots,6$) are

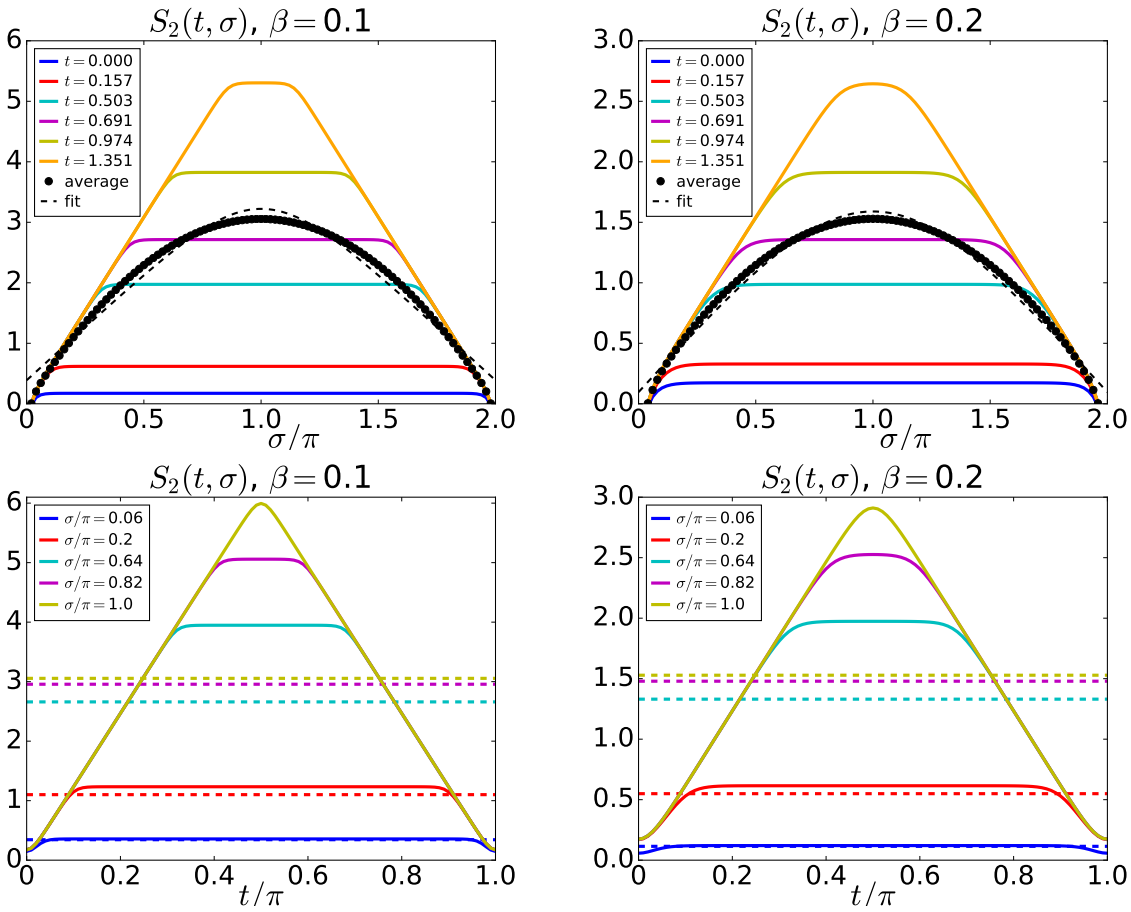

Figure 3.5: The numerical data of the $S_2(t,\sigma)$ (the second term of Eq. (3.10)). We discretize the spatial direction $\sigma \in [0, 2\pi]$ and the time direction $t \in [0, \pi]$ into 100 points ($d\sigma = 2\pi/100$ and $dt = \pi/100$). (top) σ-dependence at fixed t. The black dots are the time average of the $S_2(t,\sigma)$ from $t = 0$ to $t = \pi$. The black dashed line is the fitting of them by the formula (2.11). The left panel is for $\beta = 0.1$ and the right one is for $\beta = 0.2$. (bottom) t-dependence at fixed σ. Horizontal dashed lines indicate the time-averaged value of each colored line.

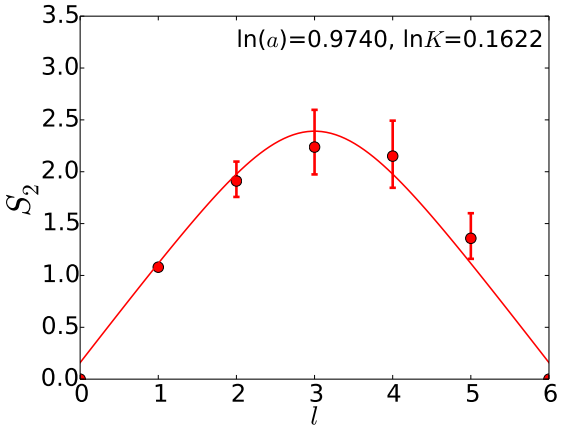

Figure 3.6: Fitting of the experiential data of the 2REE in Fig. 4A of the Ref. [12] by our formula (2.11).

used in the fitting. We do not take into account the error bar of each point in the fitting. The fitting seems well and yields $\ln(a) = 0.974$, $\ln K = 0.162$. This illustrates the validity of our formula (2.11) to the actual experimental data, although the data were obtained in a small system ($L = 6$) so it is not strongly conclusive. The applicability of the formula supports our numerical results in this chapter and provides a positive evidence for the usefulness of our formula in experiments in the near future.

In appendix B, we also give a brief result of the mutual information between two subsystems which was also measured in the experiment. We find that our analytical calculation by the cTPQ states reproduces well the experimental data of the mutual information.

3.6 Summary of this chapter

In this chapter, we find that stationary states after the quench obeys the formula (2.11) when a system is non-integrable and interacting-integrable. On the other hand, quadratic-interacting systems are not the case, and the difference between two cases are understood by the scrambling (dephasing) of a wave function during the time-evolution. Lastly we take advantage of our formula to fit the experimental data of the 2REE in ultracold atoms [12] and the agreements between the formula and the data are well.

Chapter 4

Application of the volume-law scaling formula to energy eigenstates

In this chapter, we present an application of our formula to energy eigenstates of general Hamiltonians by taking an integrable/non-integrable spin chain as an example. First we introduce the eigenstate thermalization hypothesis which claims that energy eigenstates are thermal, and explains a relation between the hypothesis and thermalization in closed quantum systems. Next we present numerical results by exact diagonalization in spin chains up to $L = 18$ sites and observe that our formula seems to apply to energy eigenstates of non-integrable systems and does not to those of integrable systems. We compare our numerical results with a recent study by Lu and Grover [68] claiming that the Rényi entanglement entropy of eigenstates of non-integrable models is not a linear function of ℓ (i.e. the volume law) and has some curvature. By checking the validity of our formula in a toy model for eigenstates of non-integrable Hamiltonians, we conclude that our formula (2.11) can work as an approximate function of the volume-law in eigenstates of non-integrable models and distinguish integrable models from non-integrable ones correctly.

4.1 Eigenstate thermalization hypothesis

Rigol *et al.* [92] proposed the Eigenstate Thermalization Hypothesis (ETH) to explain the thermalization after quantum quench in closed quantum systems. When we denote energy eigenstates of a system with energy E_α as $|\alpha\rangle$, the ETH claims [91] that for any local operator A it follows

$$A_{\alpha\beta} := \langle\alpha|A|\beta\rangle = \langle A\rangle_{\mathrm{mc},\bar{E}}\,\delta_{\alpha\beta} + e^{-S(\bar{E})/2} r_{\alpha\beta}, \tag{4.1}$$

where $\bar{E} = \frac{E_\alpha + E_\beta}{2}$, $\langle A\rangle_{\mathrm{mc},E}$ is an expectation value of A in the microcanonical ensemble at energy E, $S(E)$ is the microcanonical entropy of the system, and $r_{\alpha\beta}$ is a random fluctuation with zero mean and a variance of $O(1)$. The postulate (4.1) implies that all

energy eigenstates are thermal pure states[1] because the second term in the right hand side is exponentially small in the volume of the system.

The connection between the ETH and the thermalization after quantum quench in closed systems is formulated as follows, similar to the discussion in section 3.3. If one expand an initial state of the dynamics as $|\psi(0)\rangle = \sum_\alpha c_\alpha |\alpha\rangle$, it evolves as $\psi(t) = \sum_\alpha c_\alpha e^{-iE_\alpha t}|\alpha\rangle$. The time average leads to

$$\bar{A} = \lim_{T\to\infty} \frac{1}{T}\int_0^T ds\, \langle\psi(s)|\hat{A}|\psi(s)\rangle = \sum_\alpha |c_\alpha|^2 A_{\alpha\alpha}, \tag{4.2}$$

where we assume there is no degeneracy in the energy level spacing $E_\alpha - E_\beta$. Therefore, because the ETH (4.1) states that all energy eigenstates in the energy shell give the same expectation value $A_{\alpha\alpha}$, the thermalization occurs as $\bar{A} = \langle A\rangle_{\mathrm{mc},\bar{E}}$, as long as the initial state has a narrow distribution of $|c_\alpha|^2$, i.e., a well-defined energy. We stress that the ETH is merely a sufficient condition for the thermalization.

There are two versions of the ETH, the strong ETH and weak ETH. The strong ETH indicates a situation where all energy eigenstates of a system satisfy Eq. (4.1), while the weak ETH means that *almost* all eigenstates of a system satisfy Eq. (4.1) and that the fraction of eigenstates which does not satisfy Eq. (4.1) is vanishingly small in the thermodynamic limit. Although the strong ETH sounds too strong because it requires all eigenstates are thermal without any exception, Ref. [113] proved that the strong ETH is necessary if all product states between a subsystem and the rest of the system thermalize after quantum quench. However, the authors of Ref. [114] argued that all of those product states are not experimentally accessible and necessary to thermalize, and construct a concrete model satisfying only the weak ETH where the cTPQ states at all non-zero temperature thermalize after quantum quench. On the other hand, it is known that the weak ETH holds even in integrable systems [115]. This somewhat surprising fact can reconcile with the absence of the thermalization in integrable models in the following way: the weight $|c_\alpha|^2$ on non-thermal states which do not satisfy (4.1) dominates even though the number of such states are small [116]. In short, extent of the validity of the strong/weak ETH and its relation to the thermalization have yet to be solved (for a review, see Ref. [117]), but at least the weak ETH is believed to hold in general models.

In this chapter, we will investigate the REE of energy eigenstates in integrable/non-integrable spin chains and compare the results with our formula (2.11) derived by the cTPQ states. From the viewpoint of the ETH, this is an extension of the ETH to non-local quantities, discussed also in Refs. [57, 68, 118] (note that the REEs are highly non-local when $\ell \sim L/2$).

[1] Since A is local, the microcanonical ensemble and the canonical ensemble is equivalent in the thermodynamic limit in this equation.

4.2 Numerical calculations in spin chains

As a numerical test whether our formula applies to energy eigenstates in general systems, we study the $S = 1/2$ XXZ spin chain with/without next-nearest neighbor interactions under the periodic boundary condition,

$$H = \sum_{i=1}^{L} \left(S_i^x S_{i+1}^x + S_i^y S_{i+1}^y + \Delta S_i^z S_{i+1}^z + J_2 \boldsymbol{S}_i \cdot \boldsymbol{S}_{i+2} \right), \tag{4.3}$$

where we set $\Delta = 2$ and $J_2 = 4$ ($J_2 = 0$) for a non-integrable (integrable) case [94].

We perform exact diagonalization to this Hamiltonian and calculate the 2REE curve $S_2(\ell)$ of the eigenstates of this model with various energies (Fig. 4.1a and Fig. 4.1b). We see that the fit by the formula (2.11) works well for the non-integrable case while it does not for the integrable case. To analyze the difference between two cases quantitatively, we consider the residual of the fit divided by the system size,

$$r_i := \frac{1}{L} \sum_{\ell=1}^{L-1} \left(S_2(\ell)_{\mathrm{data},i} - S_2(\ell)_{\mathrm{fit},i} \right)^2 . \tag{4.4}$$

Here $S_2(\ell)_{\mathrm{data},i}$ is the 2REE of the i-th energy eigenstate of the system and $S_2(\ell)_{\mathrm{fit},i}$ is the fitted value of it. If $S_2(\ell)_{\mathrm{data},i} - S_2(\ell)_{\mathrm{fit},i}$ is $o(1)$ for the whole region, or the formula (2.11) fits the numerical data well, r_i tends to decrease with L. In Figs. 4.1c and 4.1d, we show the distribution of $\{r_i\}_i$ for all eigenstates in the sector of zero magnetization $\sum_i S_i^z = 0$ and zero momentum $k = 0$ by sorting them in descending order of the value r_i. It is clear that $\{r_i\}_i$ decreases with respect to L for the non-integrable case but increase for the integrable case. In Fig. 4.2, we also show the mean of $\{r_i\}$ and the decrease (increase) of the $\{r_i\}$ for the non-integrable (integrable) case is evident. Those results suggest that our formula (2.11) is applicable to eigenstates of non-integrable models but not to those of integrable models. However, we need a special care about the numerical result in non-integrable models because a recent paper by Lu and Grover [68] propose a different functional form of the nREE $S_n(\ell)$ from ours. We will discuss this point in the following section 4.3.

Before doing it, we comment on the failure of the formula in integrable models which is apparent in the numerical calculations. First, our numerical result for integrable models is consistent with a recent study by Vidmar *et. al* [119] where it was shown that the vN-EE of eigenstates of quadratic fermion models is not the same as that of the random state (thermal state at $\beta = 0$, Eq. (1.16)). Second, in terms of the "scrambling" discussed in section 2.4, the failure of our fitting function (2.11) may indicate that the off-diagonal term I_{off} is not negligible in the case of eigenstates of integrable systems. Infinitely many conserved quantities would hinder the uncorrelated nature of the coefficients $\{c_i\}$ of the wave function, for example, in the local basis. Third, it is clear from the distribution of the $\{r_i\}_i$ in Fig. 4.1 that almost all eigenstates are *violating* the formula (2.11) derived for thermal pure states. This is in stark contrast to the weak ETH concerning with local observables, where almost all eigenstates satisfy the ETH (4.1) even in integrable systems [115].

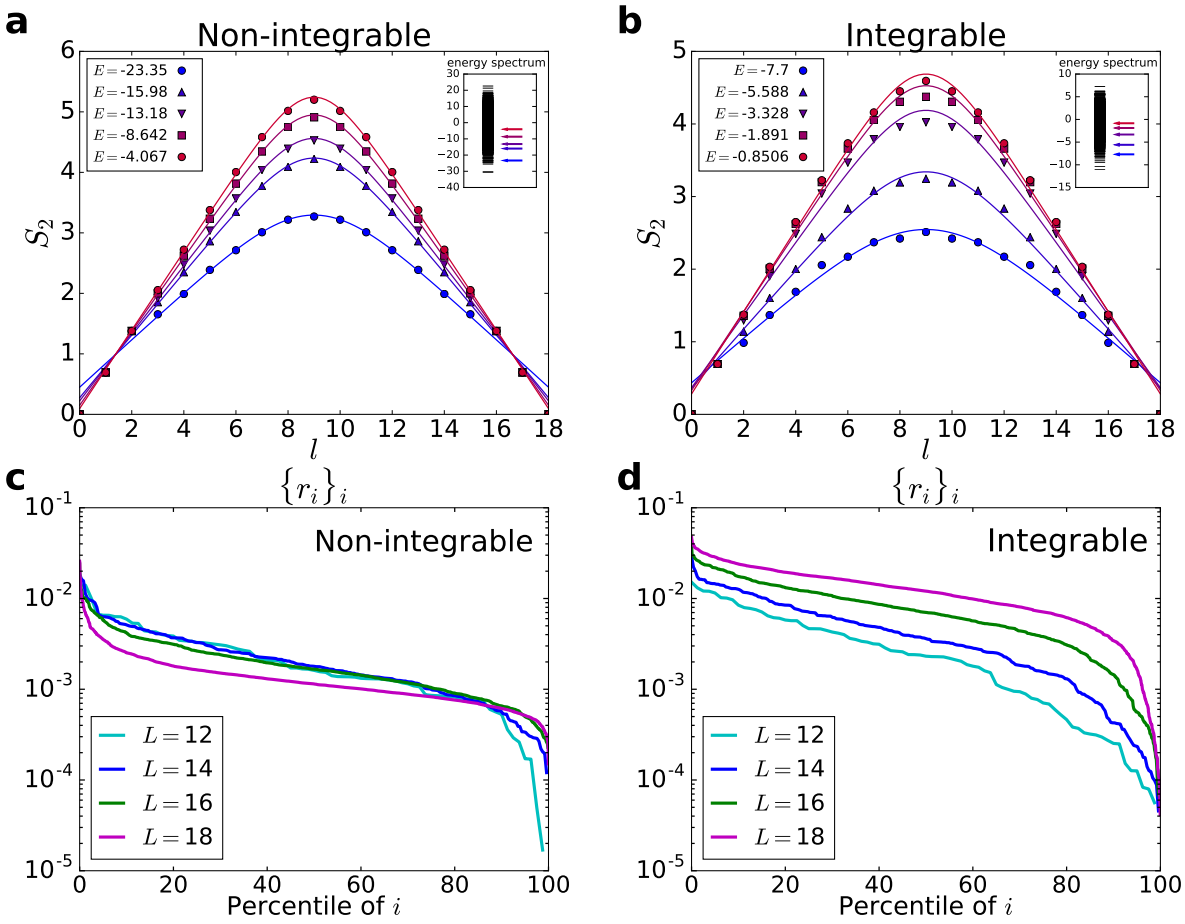

Figure 4.1: (a) The second Rényi entanglement entropy of several energy eigenstates of the non-integrable Hamiltonian, Eq. (4.3) with $L = 18$, $\Delta = 2$ and $J_2 = 4$ (dots). The fits by our formula (2.11) are also shown as lines. The inset is the energy spectrum of the Hamiltonian and the arrows indicate the eigenstates shown in the figure. (b) Same as figure (a) for the integrable Hamiltonian ($L = 18$, $\Delta = 2$, $J_2 = 0$). (c) Distribution of the residual of the fit of the i-th eigenstate, r_i (Eq. (4.4)). We plot r_i of all eigenstates of the non-integrable Hamiltonian (Eq. (4.3) with $L = 18$, $\Delta = 2$ and $J_2 = 4$) in the sector of zero momentum and total magnetization. The residuals $\{r_i\}$ are sorted in descending order, and the horizontal axis represents their percentiles. (d) Same as figure (c) for the integrable Hamiltonian ($L = 18$, $\Delta = 2$, $J_2 = 0$).

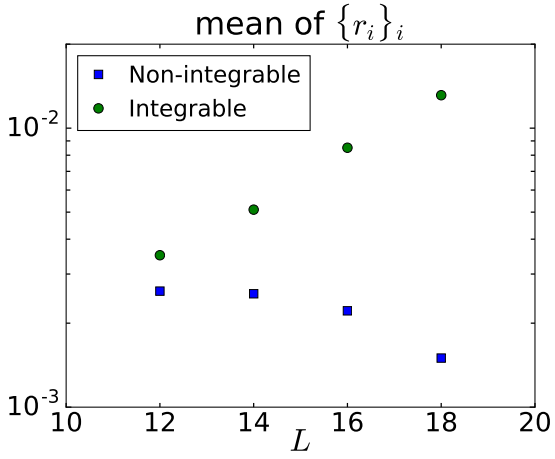

Figure 4.2: The mean of $\{r_i\}$ presented in Fig. 4.1c and Fig. 4.1d.

4.3 More analysis to non-integrable models: comparison with the result by Lu and Grover

4.3.1 Review of result by Lu and Grover for eigenstates of non-integrable models

In Ref. [68], Lu and Grover studied the nREE of energy eigenstates in general non-integrable systems. In particular[2] they focused on the thermodynamics limit where $L \to \infty$ with a non-zero fixed fraction of the subsystem, $f := \ell/L \neq 0$. As a model of energy eigenstates, they took the following "ergodic bipartite (EB) state" introduced in Refs. [36, 37],

$$|E\rangle_{EB} := \sum_{E_i^A + E_j^B \in (E-\delta/2, E+\delta/2)} C_{ij} \, |E_i^A\rangle_A \, |E_j^B\rangle_B \,, \tag{4.5}$$

where E is the total energy of eigenstate, $|E_i^{A(B)}\rangle_{A(B)}$ is an energy eigenstate of the Hamiltonian on subsystem $A(B)$ with energy $E_i^{A(B)}$ ($H = H_A + H_B + H_{\rm int}$), δ is a width of the energy shell, and $\{C_{ij}\}$ are random complex numbers taken uniformly from the unit sphere $\sum_{ij} |C_{ij}|^2 = 1$. When the eigenstates $|E_i^{A(B)}\rangle_{A(B)}$ satisfy the ETH within each subsystem $A(B)$, the EB state is proved to reproduce expectation values of any local operator taken by the microcanonical ensemble (1.10) of the total system; that is, the EB state is a thermal pure state [68].

Lu and Grover calculated the random average of nREE of the EB state, $S_{n,EB} := \frac{1}{1-n} \ln \overline{{\rm tr}_A({\rm tr}_B \, |E\rangle_{EB} \, \langle E|_{EB})^n}$. The result for the second REE is

$$S_{2,EB} = -\ln \left(\frac{\sum_{E_A} e^{S_A(E_A)+2S_B(E-E_A)} + e^{2S_A(E_A)+S_B(E-E_A)}}{\left(\sum_{E_A} e^{S_A(E_A)+S_B(E-E_A)}\right)^2} \right). \tag{4.6}$$

[2] We treat only a case of one-dimensional systems for simplicity, although their results as well as ours are not limited to one-dimensional systems.

Here the number of states in the energy shell (i.e. density of states) is denoted as e^{S_A}, so that $S_A(E_A)$ is a microcanonical entropy of the subsystem A at the subsystem energy E_A. Furthermore, for general n in the thermodynamic limit $L \to \infty$ with $f < 1/2$, their result reduces to

$$S_{n,EB} = \frac{1}{1-n} \ln \left(\frac{\sum_{E_A} e^{S_A(E_A)+nS_B(E-E_A)}}{\left(\sum_{E_A} e^{S_A(E_A)+S_B(E-E_A)}\right)^n} \right). \tag{4.7}$$

By employing intensive quantities like

$$u := E/L, \quad u_A := E_A/\ell, \quad u_B := \frac{-fu_A + u}{1-f}, \quad s(E_A) := S_A(E_A)/\ell,$$

the above equation can be rewritten as

$$S_{n,EB} = \frac{1}{1-n} \ln \left(\frac{\sum_{u_A} e^{L(fs(u_A)+n(1-f)s(u_B))}}{\left(\sum_{u_A} e^{L(fs(u_A)+(1-f)s(u_B))}\right)^n} \right). \tag{4.8}$$

Both the numerator and the denominator can be evaluated by the saddle point method when $L \to \infty$. The saddle point equation for the numerator is

$$\left.\frac{\partial s(y)}{\partial y}\right|_{y=u_A^*} = n \left.\frac{\partial s(y)}{\partial y}\right|_{y=u_B^*:=(-fu_A^*+u)/(1-f)}, \tag{4.9}$$

while that for the denominator is

$$\left.\frac{\partial s(y)}{\partial y}\right|_{y=u_A^{**}} = \left.\frac{\partial s(y)}{\partial y}\right|_{y=u_B^{**}:=(-fu_A^{**}+u)/(1-f)}, \tag{4.10}$$

which has a trivial solution $u_A^{**} = u_B^{**} = u$ for any f. With the solution u_A^* of the saddle point equation (4.9), the final result is

$$S_{n,EB} = \frac{\ell}{1-n} \left(fs(u_A^*) + n(1-f)s(u_B^*) - ns(u) \right). \tag{4.11}$$

This is one of the main results in Ref. [68]. We note that the above calculations are quite similar to ours using the cTPQ states, as seen in apparent resemblance of Eq. (4.6) to Eq. (2.7). In addition, it is worthwhile to note that Eq. (4.11) coincides with our formula (2.11) in the limit of $f \to 0$ [68].

The most important finding by them relevant to our results is the non-zero curvature of the REE curve. They showed that the density of the REE, $\tilde{s}_n(f) = \lim_{\substack{\ell,L\to\infty \\ 0<f=\ell/L<1}} S_n(\ell)/L$ is a concave (convex) function of f for $n \geq 1$ ($n \leq 1$),

$$\frac{d^2\tilde{s}_n(f)}{df^2} > 0 \quad (n > 1), \qquad \frac{d^2\tilde{s}_n(f)}{df^2} < 0 \quad (n < 1). \tag{4.12}$$

This equation indicates that our fitting function (2.11), which gives a linear dependence $\tilde{s}_2(f) = (\ln a)f$ for $f \leq 1/2$, would not be suitable to the eigenstates of non-integrable

Hamiltonians, contradicting our numerical calculation in the previous section. We think that the reason for the discrepancy is simply due to the finite size effect of the numerical calculation. In the thermodynamic limit $L \to \infty$ with fixed $f = \ell/L$, Eq. (4.12) is correct and our fitting function will not work in a strict sense. However, as already presented in Fig. 4.1a, the numerical data of the 2REE for the finite size system ($L = 18$) look *convex* rather than *concave*, suggesting that the finite size effect is too strong to see the curvature (4.12) in numerically-accessible finite systems ($L \sim 20 - 30$). Therefore we can expect that our formula (2.11) is still meaningful in finite size systems as a reasonable approximation to the 2REE curve. We examine this statement in the next subsection.

Before doing it, we comment on the derivation of Eq. (4.12). In the derivation, the calculation of the curvature reduces to the following equation:

$$\frac{d^2\tilde{s}_n(f)}{df^2} \propto (n-1)\cdot(u_A^* - u_B^*).$$

Generally, the saddle point equation (4.9) has a solution with $u_A^* \neq u_B^*$, which results in the non-zero curvature of the REE curve. However, the solution with $u_A^* \neq u_B^*$ means that the energy density of the subsystem A is different from that of the subsystem B, or the temperatures of A and B are different each other. This situation is not physical if the system is in thermal equilibrium. We think the solution with $u_A^* \neq u_B^*$ is merely a mathematical artifact and does not have any physical meaning since it depends on the index n of Rényi entanglement entropy and the fraction of the subsystem $f = \ell/L$. However, we admit the possibility that the EB state (or a single energy eigenstate) is not suitable to describe thermal equilibrium for non-local quantities such as nREE.

4.3.2 Numerical calculation in Gaussian density-of-states model

Lu and Grover [68] also studied the Gaussian density-of-states (G-DOS) model as an analytically-solvable example of their formula (4.11). Here we investigate the G-DOS model as a concrete platform for comparing the result by the cTPQ states with that by the EB states.

The G-DOS model is defined through the microcanonical entropy density,

$$s(u) = \ln 2 - \frac{1}{2}u^2. \tag{4.13}$$

The inverse temperature is $\beta = \frac{\partial s(u)}{\partial u} = -u$. This model can be considered as a good approximation to general models which satisfies $s(u) = s(-u)$ around infinite temperature [68]. Lu and Grover derived the exact results of the 2REE for this model by analytically solving the saddle point equation (4.9),

$$S_{2,GDOS}(\ell) = -\ln\left(\frac{1}{\sqrt{1-f^2}}e^{-L\gamma(u,f)} + \frac{1}{\sqrt{1-(1-f)^2}}e^{-L\gamma(u,1-f)}\right), \tag{4.14}$$

$$\gamma(u,f) = f\ln 2 - \frac{f}{1+f}u^2. \tag{4.15}$$

In top panels of Fig. 4.3, we plot the above function $S_{2,GDOS}(\ell)$ for $\beta = -u = 0.3$ and 0.6. The concave nature of the curve is observed for $\beta = 0.6$ with $L \gtrsim 18$, but hardly

visible for $\beta = 0.3$. We perform the fitting to those numerical data by our formula (2.11) (drawn as line in the figures) and calculate the residual of the fit (Eq. (4.4)). The middle panels of Fig. 4.3 show the dependence of the residual to L, which is found to be proportional to L^2. This is because $S_2(\ell)_{\rm data} - S_2(\ell)_{\rm fit}$ becomes $O(\ell)$ due to the curvature (4.12), so the $r = L^{-1}\sum_{\ell=1}^{L-1}\left(S_2(\ell)_{\rm data} - S_2(\ell)_{\rm fit}\right)^2$ becomes $L^{-1} \times L \times O(L^2) = O(L^2)$.

The most important numerical finding is in the bottom panels of Fig. 4.3. We compare the fitted values of $\ln a$ with the density of the 2REE for half of the system, $S_2(L/2)/(L/2)$. As clearly seen in the figures, those two quantities exhibit almost the same extrapolation for $1/L \to 0$, but $\ln a$ converges faster than $S_2(L/2)/(L/2)$. This observation indicates that $\ln a$ obtained by the fitting by our formula is a nice estimation of the 2REE density for half of the system in the thermodynamic limit, $\tilde{s}(1/2) = \lim_{L\to\infty} S_2(L/2)/(L/2)$. We ascribe the reason why $\ln a$ can extract the density $\tilde{s}(1/2)$ correctly to the following two points. First, the fitting by our formula which is basically a linear function of f will yield the average slope of the (nonlinear) REE curve of energy eigenstates as $\ln a$, and the density of the 2REE $\tilde{s}(1/2)$ is a reasonable candidate for such average slope. Second, the curvature $d^2\tilde{s}(f)/df^2$ turns out to be large at small f and $1-f$ as seen in the top right panel of Fig. 4.3, so that the fitting by the (linear) function (2.11) might prefer the region around $f = 1/2$ and extract information there. In short, we claim that the fitting by our formula (2.11) applies approximately to energy eigenstates of non-integrable models and is still useful in numerical calculation in practice.

Finally, we stress that the failure of the formula (2.11) for the integrable model in section 4.2 is clearly valid since the residual $\{r_i\}$ grows exponentially in L there, in contrast to the $O(L^2)$ growth of the G-DOS model. In other words, the fitting by our formula can tell the integrable model from the non-integrable model.

4.3.3 Origin of difference between the cTPQ state and the EB state

We discuss the reason for the different functional forms of the 2REE between the cTPQ states (2.11) and the EB states (4.11), (4.12).

From the viewpoint of "scrambling" discussed in section 2.4, the different functional form of the EB states comes from absence of the extensiveness of the diagonal ensemble in Eq. (2.17) (the condition (2) in section 2.4). The diagonal ensemble of the EB state after random average is

$$\hat{\rho}_{{\rm dia},EB} = \frac{1}{N} \sum_{E_i^A + E_j^B \in (E-\delta/2, E+\delta/2)} |E_i^A\rangle_A |E_j^B\rangle_B \langle E_i^A|_A \langle E_j^B|_B , \tag{4.16}$$

and the 2REE curve of the EB state (4.6) can be reproduced by plugging in the above expression into Eq. (2.17). We note that the off-diagonal contribution $I_{\rm off}$ is again absent after the random average. Therefore, the nonlinear property of the 2REE curve of the EB states traces back to a nonlinear extensiveness of the diagonal ensemble $\hat{\rho}_{{\rm dia},EB}$,

$$\mathrm{tr}_A\left(\mathrm{tr}_B\left(\hat{\rho}_{{\rm dia},EB}\right)^2\right) \approx c \cdot \left(a_{\ell/L}\right)^{-\ell}, \ \mathrm{tr}_B\left(\mathrm{tr}_A\left(\hat{\rho}_{{\rm dia},EB}\right)^2\right) \approx c \cdot \left(a_{\ell/L}\right)^{-L+\ell}, \tag{4.17}$$

where $a_{\ell/L}$ depends on the fraction of the subsystem ℓ/L.

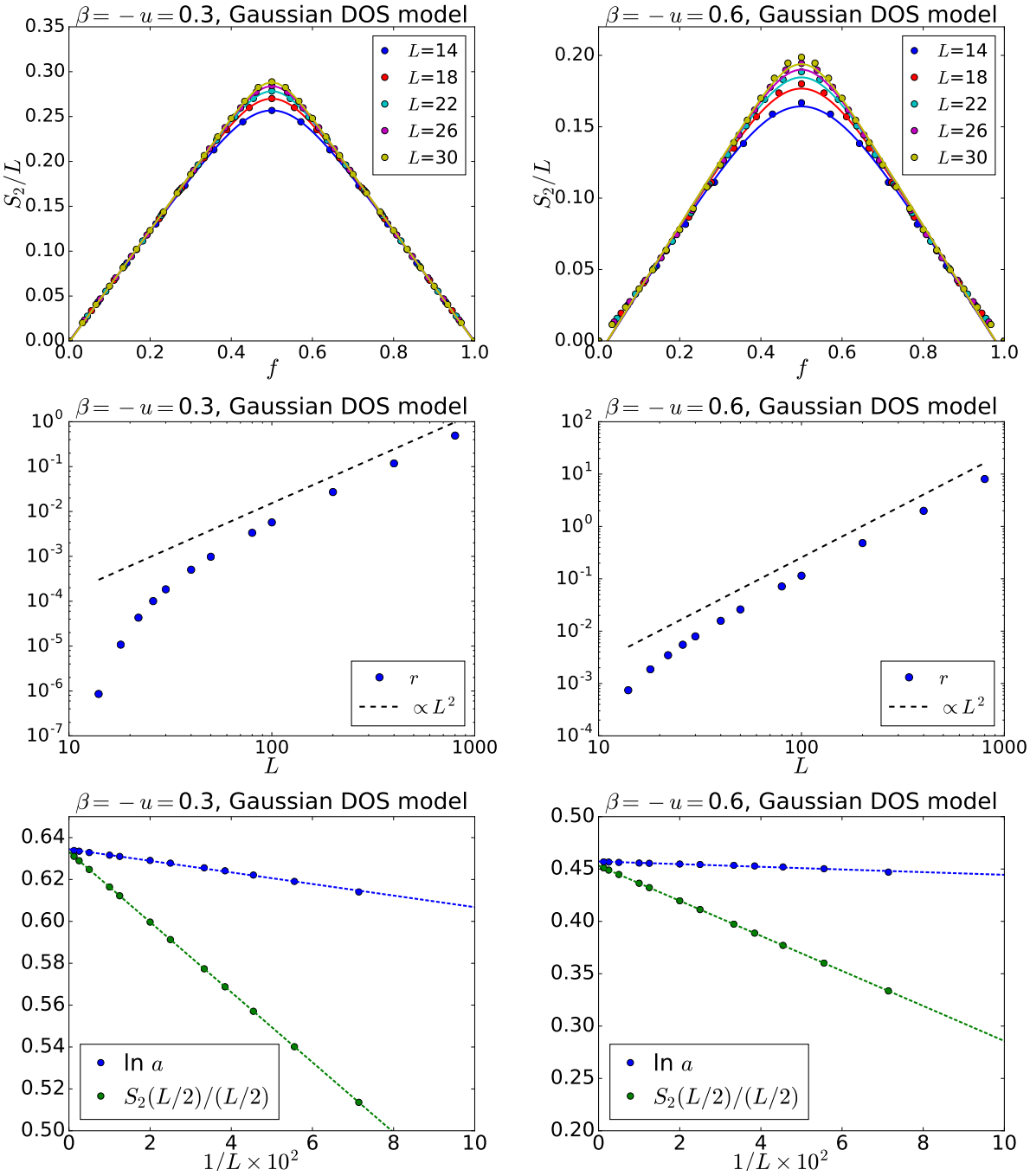

Figure 4.3: Numerical result of the 2REE of the G-DOS model at $\beta = 0.3$ (left panels) and $\beta = 0.6$ (right panels). (top) Dots are the 2REE of the G-DOS model (Eq. (4.14)) and lines are the fit of them by our formula (2.11). The horizontal axis is $f = \ell/L$. (middle) The residual of the fit defined in Eq. (4.4). The dashed line is a guide for eyes which is proportional to L^2. (bottom) Comparison between the fitted slope of the curve, ln a, and the density of the 2REE for half of the system, $S_2(L/2)/(L/2)$. The dashed lines are linear extrapolations to $1/L \to 0$.

The reason for this surprising nonlinearity has not been understood clearly, but from the viewpoint of energy variance in the total system $\langle (H - \langle H \rangle)^2 \rangle$, it might be rather a special feature of a *single* eigenstate. A single eigenstate by definition has no energy variance $\langle (H - \langle H \rangle)^2 \rangle = 0$, while the usual microcanonical ensemble (1.10) has energy variance of $O(\delta^2)$. Indeed, energy variance of the EB state after random average is $\langle (H - \langle H \rangle)^2 \rangle_{EB} \propto f(1-f)L$, which is zero for $f = 1$ (where the subsystem A becomes the total system). Although the EB state and a single eigenstate correspond to the microcanonical ensemble in terms of the definition of thermal pure states in section 1.2, energy variance of such eigenstates is different from that of the microcanonical ensemble with a non-zero width of the energy shell. On the other hand, if one employs a *superposition* of energy eigenstates in the energy shell rather than a single eigenstate like the EB state, the superposed state is still a thermal pure state and has non-zero of energy variance. The calculation of the 2REE for that superposed state, however, may not proceed in parallel to the derivation of Eq. (4.11) because the finite energy variance might affect, for example, the expression (4.6) and its thermodynamics limit (4.8). In that case we expect the 2REE curve becomes close to our formula (2.11). We admit that the discussion in this paragraph is heuristic, and the explicit calculation of the 2REE of the superposed state would be an interesting direction for future study.

Lastly, we point out that stationary states after quantum quench usually correspond to the microcanonical ensemble with a non-zero width of the energy shell or possibly the canonical ensemble (the Gibbs state). This is because energy variance of typical initial states which are accessible by experiments is large ($O(L)$ for the cTPQ states and the Gibbs state) and the energy variance is consevered during time-evolution (a related discussion is found in Ref. [57]). Energy variance of the Néel state which we considered in Chapter 3 is $O(L)$ in the model (3.3) and actually the energy distribution of the Néel state is broad [101]. Therefore, we claim that the 2REE of the stationary states after the quench from the Néel state is described by our formula (2.11).

4.4 Summary of this chapter

In this chapter we study the 2REE of energy eigenstates of integrable and non-integrable spin chains. Our numerical results by exact diagonalization suggest that the 2REE of the non-integrable model exhibits the volume law of the form of Eq. (2.11) whereas that of the integrable model does not. We also compare our numerical result with a recent result for eigenstates in non-integrable systems [68] which showed that the slope of the volume law, $\lim_{\ell\to\infty} S_2(\ell)/\ell$, is not constant while our formula (2.11) gives a constant value to it. By numerically examining an analytically solvable toy model, we find that the fitting by our formula is still meaningful to energy eigenstates in the sense that (1) it can correctly distinguish integrable models from non-integrable ones and (2) it is a nice approximation to the actual 2REE curve in non-integrable models and extracts the density of the 2REE for half of the system well.

Chapter 5

Summary and Conclusion

In this thesis, we study the volume law of entanglement mainly focusing on the second Rényi entanglement entropy for thermal pure states.

In Chapter 2, an analytical formula of the volume law scaling is derived by employing the cTPQ states. The whole curve, including the deviation from a linear volume law scaling $S_2 \propto \ell$, is determined by only two parameters: the 2REE density $\ln a$ and the offset $\ln K$ (Eq. (2.11)). We illustrated a practical advantage of the formula by numerically computing the 2REE of the cTPQ states and fitting it by the formula. The formula extracts the density of the 2REE more accurately than other naive ways based on the linear volume law. Furthermore, we discuss the universality of the formula by considering the scrambling, or dephasing, of wave functions of general pure states. We conjecture that our formula of the 2REE will apply to various scrambled pure states, which include thermal pure states.

In Chapter 3, we study the 2REE of stationary pure states after quantum quench by numerical exact diagonalization. The 2REE of the stationary states in non-integrable models exhibits the volume law of the form (2.11). Somewhat surprisingly, the formula, which is derived by the cTPQ states (thermal states), is shown to apply also to interacting-integrable models where there is no thermalization. Those results are understood by the "scrambling" of the wave function during time-evolution, along with a numerical result for quadratic-integrable models where there is no scrambling at all. Finally, we perform the fitting of the experimental data of the 2REE in ultracold atoms [12], which works quite well.

In Chapter 4, energy eigenstates in general integrable/non-integrable systems are investigated. We again employ the exact diagonalization and calculate the 2REE of eigenstates numerically. Our numerical results suggest that the 2REE of non-integrable models obeys Eq. (2.11) while that of integrable models does not. Although a recent study [68] derived the different functional form of the volume law for energy eigenstates of non-integrable models as ours, our formula (2.11) is still meaningful in extracting information of the system in the thermodynamic limit from finite size systems and telling non-integrable models from integrable models.

The result in this thesis will contribute to link quantum mechanics with thermodynamics, whose connection is a long-standing problem since the early days of the discovery of quantum mechanics. Our formula (2.11) and its universality in many kinds of thermal

pure states have a lot of implications. First, our formula (2.11) tells that the deviation from the linear volume law $S_2(\ell) \propto \ell$ is at most $O(1)$ at general finite temperatures, which means that the density of the 2REE $\lim_{\ell\to\infty} S_2(\ell)/\ell$ of thermal pure states is exactly the same as that of (if any) thermal ensemble. This is an extension of the previous studies of the pure state thermodynamics to one of the most important non-local quantities in quantum many-body systems; the REE. Second, the applicability of our formula to stationary states after quantum quench demonstrated in Chapter 3 offers a way to investigate the "scrambling" of a given initial state in closed quantum systems. The fitting of the REE curve $S_2(t, \ell)$ at each time t will give a criterion for the system to "scramble", a cousin of the thermalization. The result in Chapter 3 can also be seen as a non-local extension of the studies on the thermalization in the previous literature. Third, the formula gives an accurate prediction of the density of the 2REE in the thermodynamics limit from a result in finite size systems. This is definitely of use in numerical/experimental studies on the entanglement entropy in the future.

As a future direction, it is interesting to compute the functional form of the vN-EE $S_1(\ell)$, which is directly related to thermal entropy of a system, by finding an expression of the nREE for general integers $n = 2, 3, \cdots$. Another interesting direction is to apply our formula to various topics in quantum many-body systems related to the REE. For example, chaos in quantum systems that is known to have a deep connection to the out-of-time-order correlations [65–67] can be examined by the 2REE in some setup [64]. Since our result is quite fundamental in that it just gives a functional form of the volume law of the REE for generic thermal (as well as scrambled) pure states, we hope the applications of it will be diverse.

Appendix A

Proof on the difference between $\overline{S_n}$ and $\tilde{S}_n$

In this appendix we prove the following property of the cTPQ states mentioned in section 2.2:

$$\overline{\ln\left[\mathrm{tr}_A\left(\rho_A^n\right)\right]} = \ln\overline{\left[\mathrm{tr}_A\left(\rho_A^n\right)\right]} + O(e^{-L}), \tag{A.1}$$

where $\overline{\cdots}$ is random average over the coefficients $\{z_i\}$ of the cTPQ states and L is the system size. This property justifies our derivation of the formula (2.11) where we substitute $\overline{\ln\left[\mathrm{tr}_A\left(\rho_A^n\right)\right]}$ for $\ln\overline{\left[\mathrm{tr}_A\left(\rho_A^n\right)\right]}$. First we provide a (non-rigorous) sketch of the proof of the above equation and then we give a more rigorous proof which is rather technical. We note that a proof on the same statement for the EB states (Eq. (4.5)) is provided in Ref. [68].

A.1 Sketch of the proof

Let us set up definitions and notations. We assume that n is integer satisfying $n \geq 2$. We denote $W[z, z^*] := \mathrm{tr}_A\left(\rho_A^n\right)$, where $z = \{z_i\}$ are the random complex numbers whose real and imaginary parts are taken from the normal distribution $\mathcal{N}(0, 1/\sqrt{2})$. We write the random number average of $W[z, z^*]$ over z as $\Omega := \overline{W[z, z^*]}$. Then what to prove is

$$\overline{\ln W[z, z^*]} = \ln\Omega + O(e^{-L}) \iff \overline{\ln\left[\frac{W[z, z^*]}{\Omega}\right]} = O(e^{-L}). \tag{A.2}$$

Now we *formally* expand the logarithm around $\frac{W[z,z^*]}{\Omega} = 1$ and obtain

$$\overline{\ln\left[\frac{W[z, z^*]}{\Omega}\right]} = -\frac{1}{2}\overline{\left(\frac{W[z, z^*]}{\Omega} - 1\right)^2} + \frac{1}{3}\overline{\left(\frac{W[z, z^*]}{\Omega} - 1\right)^3} - \frac{1}{4}\overline{\left(\frac{W[z, z^*]}{\Omega} - 1\right)^4} + \cdots, \tag{A.3}$$

where we used $\overline{\frac{W[z,z^*]}{\Omega}} = 1$. The first term $\overline{\left(\frac{W[z,z^*]}{\Omega} - 1\right)^2}$ can be written as

$$\overline{\left(\frac{W[z, z^*]}{\Omega} - 1\right)^2} = \frac{\overline{W^2} - \Omega^2}{\Omega^2}. \tag{A.4}$$

By directly calculating the random average, one can show that $\overline{W^2} - \Omega^2$ is $\Omega^2 \times O(e^{-L})$. Likewise, the term $\overline{(W-\Omega)^m}$ scales as

$$\frac{\overline{(W-\Omega)^m}}{\Omega^m} = O(e^{-\lfloor m/2 \rfloor L}), \tag{A.5}$$

as explained in section A.3. Therefore, by summing up all the contributions in Eq. (A.3), we reach

$$\overline{\ln\left[\frac{W[z,z^*]}{\Omega}\right]} = \sum_{k=1}^{\infty} a_k e^{-kL}, \tag{A.6}$$

where a_k is independent of L and scales at most exponentially in k because it comes from combinatorial numbers appearing in contracting the random numbers z (see also discussions in section A.3). For sufficiently large L, the right hand side of the above equation converges, which is order of $O(e^{-L})$.

A.2 More rigorous Proof

The above argument is not mathematically rigorous because there is always a chance that $\frac{W[z,z^*]}{\Omega}$ becomes larger than two, which is out of the convergence radius of the logarithm (note that the random number z is taken from the normal distribution). In this section we provide a proof with taking care of this point.

We introduce the probability distribution for $\Phi := W[z,z^*]/\Omega$ as $P[\Phi]$, so that we have

$$\overline{\ln\left[\frac{W[z,z^*]}{\Omega}\right]} = \int_{1/d_A^{n-1}}^{d_A^{n-1}} d\Phi P[\Phi] \ln \Phi. \tag{A.7}$$

Here the range of integration is taken as $\left[1/d_A^{n-1}, d_A^{n-1}\right]$ since $1/d_A^{n-1} \leqslant \mathrm{tr}_A\left(\rho_A^n\right) \leqslant 1$ holds by construction, where d_A is the dimension of the subsystem A, and therefore $1/d_A^{n-1} \leqslant \Phi \leqslant d_A^{n-1}$ follows. We assume the subsystem A is smaller than the subsystem B (when A is larger than B then the bound is given by d_B and the proof goes in parallel). Next we expand $\ln \Phi = (\Phi - 1) - (\Phi - 1)^2/(2\xi^2)$, where ξ takes a value between 1 and Φ (the Taylor 's theorem),

$$\overline{\ln \Phi} = \int_{1/d_A^{n-1}}^{d_A^{n-1}} d\Phi P[\Phi](\Phi - 1) - \frac{1}{2}\int_{1/d_A^{n-1}}^{d_A^{n-1}} d\Phi P[\Phi]\frac{(\Phi-1)^2}{\xi^2}, \tag{A.8}$$

but the first term gives zero because $\overline{\Phi - 1} = 0$. In the following, we evaluate the second term by dividing the range of integration into two parts, $[1/d_A^{n-1}, 1/2]$ and $[1/2, d_A^{n-1}]$.

Integration range $[1/d_A^{n-1}, 1/2]$. First we evaluate

$$J_1 := \int_{1/d_A^{n-1}}^{1/2} d\Phi P[\Phi]\frac{(\Phi-1)^2}{\xi^2} \quad \geq 0. \tag{A.9}$$

Since $\xi \geq 1 > 1/d_A^{n-1}$ we have

$$J_1 < \int_{1/d_A^{n-1}}^{1/2} d\Phi P[\Phi] d_A^{2(n-1)} (\Phi - 1)^2, \tag{A.10}$$

and also because $(\Phi - 1)^2 < 1$ in the range of integration, it follows that

$$J_1 < \int_{1/d_A^{n-1}}^{1/2} d\Phi P[\Phi] d_A^{2(n-1)} (\Phi - 1)^2 < d_A^{2(n-1)} \int_{1/d_A^{n-1}}^{1/2} d\Phi P[\Phi]. \tag{A.11}$$

The rightmost expression has an upper bound by the Chebyshev inequality for higher moments. The inequality on the $2n$-th moment states that Prob $(|\Phi - 1| > 1/2) \leq 2^{2n} \overline{(\Phi - 1)^{2n}}$, so we obtain

$$J_1 < d_A^{2(n-1)} \times 2^{2n} \overline{(\Phi - 1)^{2n}}. \tag{A.12}$$

From Eq. (A.5), it follows that $\overline{(\Phi - 1)^{2n}} = O(e^{-nL})$. In addition, the assumption that the subsystem A is smaller than B means $d_A \leq O(e^{L/2})$. Hence the right hand side of the above inequality is $O(e^{-L})$.

Integration range $[1/2, d_A^{n-1}]$. What to evaluate is

$$J_2 := \int_{1/2}^{d_A^{n-1}} d\Phi P[\Phi] \frac{(\Phi - 1)^2}{\xi^2} \quad \geq 0. \tag{A.13}$$

From $\xi > 1/2$ we have

$$J_2 < 4 \int_{1/2}^{d_A^{n-1}} d\Phi P[\Phi] (\Phi - 1)^2. \tag{A.14}$$

Since the integrand is positive, it is possible to enlarge the range of integration,

$$J_2 < 4 \int_{1/2}^{d_A^{n-1}} d\Phi P[\Phi] (\Phi - 1)^2 \leq 4 \int_{1/d_A^{n-1}}^{d_A^{n-1}} d\Phi P[\Phi] (\Phi - 1)^2 = 4 \overline{(\Phi - 1)^2}. \tag{A.15}$$

The right hand side is $O(e^{-L})$ from Eq. (A.5).

Finally, by summing up the above two results, we reach

$$\overline{\ln \Phi} = O(e^{-L}), \tag{A.16}$$

which is the desired result.

A.3 Proof of Eq. (A.5)

Here we explain about Eq. (A.5) whereas a proof of it for general m and n is fairly complicated. The proof proceeds in the same way as in computing $\tilde{S}_n$ in section 2.2, i.e., just contracting a lot of random numbers $\{z_i\}$.

Like Eq. (2.5), we write

$$\overline{(\mathrm{tr}_A\,\rho_A^n-\Omega)^m} = \prod_{\alpha=1}^{m}\left(\frac{1}{Z(\beta)^n}\sum_{\substack{i^{(\alpha)}j^{(\alpha)}\\ a^{(\alpha)}b^{(\alpha)}}} z_{i_1^{(\alpha)}}z^*_{j_1^{(\alpha)}}\cdots z_{i_n^{(\alpha)}}z^*_{j_n^{(\alpha)}}\,\langle a_1^{(\alpha)}b_1^{(\alpha)}|e^{-\beta H/2}|i_1^{(\alpha)}\rangle\cdots\langle j_n^{(\alpha)}|e^{-\beta H/2}|a_1^{(\alpha)}b_n^{(\alpha)}\rangle-\Omega\right).$$

The random average is performed by contracting pairs of z and z^* (recall that $\overline{z_i z_j^*}=\delta_{ij}$ and so on) in the above expression, which results in a lot of different terms corresponding to many combinatorial ways of the contraction. Since $\Omega=\overline{W[z,z^*]}=\overline{(\mathrm{tr}_A\,\rho_A^n)}$, the terms which survive come from contractions where al least one of $z_{i^{(\alpha)}}$ (or $z^*_{j^{(\alpha)}}$) is contracted to $z^*_{j^{(\beta)}}$ (or $z_{i^{(\beta)}}$) with $\alpha\neq\beta$. However, the order of such terms is smaller than the order of Ω^m by at least $O(e^{-\lfloor m/2\rfloor L})$. A naive way to understand this is that the degrees of freedom in the indices of the sum significantly decrease in such contractions. When computing $\Omega^m=\sum_{a,b}(\cdots)$, the indices (a,b) of the summation run for $(\ell^n(L-\ell)^n)^m$ combinations. On the other hand, when computing the terms which contain "bridging" contractions between α and β ($\alpha\neq\beta$), the indices run for $\ell^{mn-c}(L-\ell)^{mn-c'}$ combinations, where c and c' are some integers (≥ 1) dependent on the way of the contractions. This means that the order of the latter terms is smaller than that of the former ones. Actually, among all terms in $\overline{(\mathrm{tr}_A\,\rho_A^n-\Omega)^m}$, the largest contribution will come from the ones in

$$\begin{aligned}&\overline{(\mathrm{tr}_A\,\rho_A^n-\Omega)^2}\times\overline{(\mathrm{tr}_A\,\rho_A^n-\Omega)^2}\times\cdots\times\overline{(\mathrm{tr}_A\,\rho_A^n-\Omega)^2}\ \ (m\text{ is even})\\ &\overline{(\mathrm{tr}_A\,\rho_A^n-\Omega)^3}\times\overline{(\mathrm{tr}_A\,\rho_A^n-\Omega)^2}\times\cdots\times\overline{(\mathrm{tr}_A\,\rho_A^n-\Omega)^2}\ \ (m\text{ is odd}),\end{aligned}$$

which is order of $\Omega^m\times O(e^{-\lfloor m/2\rfloor L})$.

For example, for $n=2$ and $m=2$, $\overline{(W[z,\bar{z}]-\Omega)^m}$ contains

$$\begin{aligned}&\frac{1}{Z(\beta)^4}\times\big(Z_A(\beta)^2Z_A(2\beta)Z_B(4\beta),\ Z_A(4\beta)Z_B(\beta)^2Z_B(2\beta),\\ &Z_A(\beta)Z_A(3\beta)Z_B(\beta)Z_B(3\beta),\ Z_A(2\beta)^2Z_B(2\beta)^2,\ Z_A(4\beta)Z_B(4\beta)\big),\end{aligned}$$

whereas $\Omega^m=\frac{1}{Z(\beta)^4}\left(Z_A(\beta)^2Z_B(2\beta)+Z_A(2\beta)Z_B(\beta)^2\right)^2$. Here we assume $e^{-\beta H}\approx e^{-\beta H_A}\cdot e^{-\beta H_B}$ as in the same sprit of the approximations (2.9). One can tell that all terms of $\overline{(W[z,\bar{z}]-\Omega)^m}$ are of the order of $\Omega^m\times O(e^{-L})$ in this example.

A.4 Numerical comparison of $\overline{S_2}$ and $\tilde{S}_2$

Finally, we present numerical results on the difference between $\overline{S_2}$ and $\tilde{S}_2$ just for illustration. We take the XX chain (2.15) in Chapter 2 as an example and calculate both $\overline{S_2}=-\overline{\ln(\mathrm{tr}_A\,\rho_A^2)}$ and $\tilde{S}_2=-\ln\left(\overline{\mathrm{tr}_A\,\rho_A^2}\right)$ of the (unnormalized) cTPQ state $|\phi_\beta\rangle$ at $\beta=2$. As Fig. A.1 clearly indicates, the difference between $\overline{S_2}$ and $\tilde{S}_2$ is quite small even for $L=10$ and it decays rapidly with L.

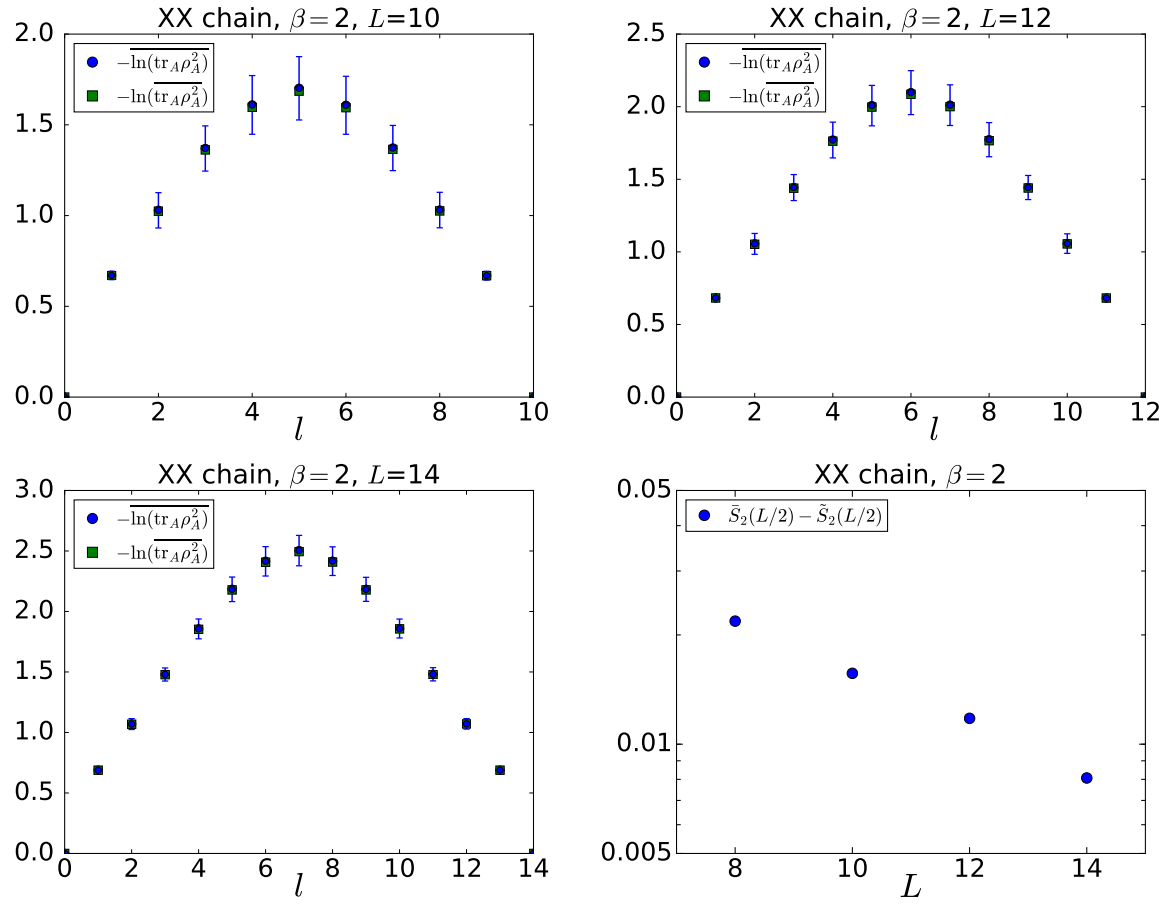

Figure A.1: (top left, top right, bottom left) Numerical result of the 2REE of the unnormalized cTPQ states $|\phi_\beta\rangle$ at $\beta = 2$ for $L = 10, 12, 14$. Blue circles are the data of $\overline{S_2} = -\overline{\ln(\mathrm{tr}_A\,\rho_A^2)}$ and green squares are those of $\tilde{S}_2 = -\ln\left(\overline{\mathrm{tr}_A\,\rho_A^2}\right)$. The random average is taken over 1000 realizations and the error bars are the standard deviations of $S_2 = -\ln(\mathrm{tr}_A\,\rho_A^2)$. (bottom right) The difference between $\overline{S_2}$ and $\tilde{S}_2$ at the center of the system $\ell = L/2$ is plotted with the system size L in semi-log scale.

Appendix B

Functional form of mutual information

Kaufman *et al.* measured the second Rényi mutual information (2RMI) between two subsystems as well as the second Rényi entanglement entropy of a single subsystem [12]. In this appendix, we derive a functional form of the 2RMI for thermal pure states and show that the qualitative behavior of that function is the same as the one observed in the experiment.

The 2RMI between two subsystems A and B is defined as

$$I_2(A,B) := S_2(A) + S_2(B) - S_2(A \cup B), \tag{B.1}$$

where $S_2(X)$ is the second Rényi entanglement entropy of a subsystem X. It is known that the mutual information can properly measure quantum correlations between two subsystems even for excited states, while the Rényi entanglement entropy does not [50]. We choose subsystems A and B which consist of $\ell_a \times M$ sites and $\ell_b \times M$ sites, respectively. We will consider both cases where A and B share a boundary (i.e. $A \cup B$ is connected) and where they do not ($A \cup B$ is disconnected). According to our result in Chapter 2, the 2REEs of these subsystems are

$$S_2(A) = -\ln(a^{-\ell_a} + a^{-L+\ell_a}) + \ln K, \tag{B.2}$$

$$S_2(B) = -\ln(a^{-\ell_b} + a^{-L+\ell_b}) + \ln K, \tag{B.3}$$

$$S_2(A \cup B) = -\ln(a^{-(\ell_a+\ell_b)} + a^{-L+(\ell_a+\ell_b)}) + (2-q)\ln K, \tag{B.4}$$

where $q = 1$ when $A \cup B$ is connected and $q = 0$ when $A \cup B$ is disconnected[1]. The 2RMI between A and B is hence written as

$$I_2 = \ln\left(\frac{a^{-(\ell_a+\ell_b)} + a^{-L+(\ell_a+\ell_b)}}{(a^{-\ell_a} + a^{-L+\ell_a})(a^{-\ell_b} + a^{-L+\ell_b})}\right) + q\ln K. \tag{B.5}$$

For simplicity, let us set $\ell_a = \ell_b = \ell/2$ where ℓ denotes a combined volume of the subsystems. The above formula reduces to

$$I_2 = \ln\left(\frac{a^{-\ell} + a^{-L+\ell}}{(a^{-\ell/2} + a^{-L+\ell/2})^2}\right) + q\ln K. \tag{B.6}$$

[1] We note that $\ln K$ comes from the boundary of the subsystem(s).

For $(1 \ll)\ \ell \ll L/2$, I_2 can be approximated as

$$I_2 \approx a^{-L+\ell} \cdot (a^\ell - 2) + q \ln K, \tag{B.7}$$

which means that I_2 grows exponentially with ℓ. For $L/2 \ll \ell\ (\ll L)$, one finds

$$I_2 \approx (2\ell - L) \ln a - 2 \ln(1 + a^{\ell - L}) + \ln(1 + a^{L-2\ell}) + q \ln K, \tag{B.8}$$

which indicates a linear growth of I_2 with ℓ. Those behaviors resemble the result of the experiment (Fig. 4C of Ref. [12]), though the experimental data were the mean of 2RMI for all configurations of the subsystems whose combined volume is ℓ.

Bibliography

[1] A. Einstein, B. Podolsky and N. Rosen. "Can Quantum-Mechanical Description of Physical Reality Be Considered Complete?" *Phys. Rev.* **47**, 777–780 (1935).

[2] E. Schrödinger. "Die gegenwärtige Situation in der Quantenmechanik". *Naturwissenschaften* **23**, 807–812, 823–828, 844–849 (1935).

[3] J. S. Bell. "On the Einstein Podolsky Rosen paradox". *Physics* **1**, 195–200 (1964).

[4] A. Aspect, P. Grangier and G. Roger. "Experimental Tests of Realistic Local Theories via Bell's Theorem". *Phys. Rev. Lett.* **47**, 460–463 (1981).

[5] A. Aspect, P. Grangier and G. Roger. "Experimental Realization of Einstein-Podolsky-Rosen-Bohm Gedankenexperiment: A New Violation of Bell's Inequalities". *Phys. Rev. Lett.* **49**, 91–94 (1982).

[6] A. Aspect, J. Dalibard and G. Roger. "Experimental Test of Bell's Inequalities Using Time-Varying Analyzers". *Phys. Rev. Lett.* **49**, 1804–1807 (1982).

[7] M. Nielsen and I. Chuang. *Quantum Computation and Quantum Information*. Cambridge Series on Information and the Natural Sciences. Cambridge University Press (2000).

[8] R. Horodecki, P. Horodecki, M. Horodecki and K. Horodecki. "Quantum entanglement". *Rev. Mod. Phys.* **81**, 865–942 (2009).

[9] N. Laflorencie. "Quantum entanglement in condensed matter systems". *Physics Reports* **646**, 1 – 59 (2016).

[10] L. Amico, R. Fazio, A. Osterloh and V. Vedral. "Entanglement in many-body systems". *Rev. Mod. Phys.* **80**, 517–576 (2008).

[11] R. Islam, R. Ma, P. M. Preiss, M. Eric Tai, A. Lukin, M. Rispoli and M. Greiner. "Measuring entanglement entropy in a quantum many-body system". *Nature* **528**, 77–83 (2015).

[12] A. M. Kaufman, M. E. Tai, A. Lukin, M. Rispoli, R. Schittko, P. M. Preiss and M. Greiner. "Quantum thermalization through entanglement in an isolated many-body system". *Science* **353**, 794–800 (2016).

[13] H. Pichler, G. Zhu, A. Seif, P. Zoller and M. Hafezi. "Measurement Protocol for the Entanglement Spectrum of Cold Atoms". *Phys. Rev. X* **6**, 041033 (2016).

[14] N. M. Linke, S. Johri, C. Figgatt, K. A. Landsman, A. Y. Matsuura and C. Monroe. "Measuring the Renyi entropy of a two-site Fermi-Hubbard model on a trapped ion quantum computer". *arXiv* 1712.08581 (2017).

[15] C. Neill, P. Roushan, M. Fang, Y. Chen, M. Kolodrubetz, Z. Chen, A. Megrant, R. Barends, B. Campbell, B. Chiaro, A. Dunsworth, E. Jeffrey, J. Kelly, J. Mutus, P. J. J. O'Malley, C. Quintana, D. Sank, A. Vainsencher, J. Wenner, T. C. White, A. Polkovnikov and J. M. Martinis. "Ergodic dynamics and thermalization in an isolated quantum system". *Nature Physics* **12**, 1037 (2016).

[16] J. Li, R. Fan, H. Wang, B. Ye, B. Zeng, H. Zhai, X. Peng and J. Du. "Measuring Out-of-Time-Order Correlators on a Nuclear Magnetic Resonance Quantum Simulator". *Phys. Rev. X* **7**, 031011 (2017).

[17] M. Srednicki. "Entropy and area". *Phys. Rev. Lett.* **71**, 666–669 (1993).

[18] J. Eisert, M. Cramer and M. B. Plenio. "*Colloquium* : Area laws for the entanglement entropy". *Rev. Mod. Phys.* **82**, 277–306 (2010).

[19] C. Holzhey, F. Larsen and F. Wilczek. "Geometric and renormalized entropy in conformal field theory". *Nuclear Physics B* **424**, 443 – 467 (1994).

[20] G. Vidal, J. I. Latorre, E. Rico and A. Kitaev. "Entanglement in Quantum Critical Phenomena". *Phys. Rev. Lett.* **90**, 227902 (2003).

[21] P. Calabrese and J. Cardy. "Entanglement entropy and quantum field theory". *Journal of Statistical Mechanics: Theory and Experiment* **2004**, P06002 (2004).

[22] P. Calabrese and J. Cardy. "Entanglement entropy and conformal field theory". *Journal of Physics A: Mathematical and Theoretical* **42**, 504005 (2009).

[23] M. M. Wolf. "Violation of the Entropic Area Law for Fermions". *Phys. Rev. Lett.* **96**, 010404 (2006).

[24] D. Gioev and I. Klich. "Entanglement Entropy of Fermions in Any Dimension and the Widom Conjecture". *Phys. Rev. Lett.* **96**, 100503 (2006).

[25] B. Swingle. "Entanglement Entropy and the Fermi Surface". *Phys. Rev. Lett.* **105**, 050502 (2010).

[26] B. Swingle. "Conformal field theory approach to Fermi liquids and other highly entangled states". *Phys. Rev. B* **86**, 035116 (2012).

[27] W. Ding, A. Seidel and K. Yang. "Entanglement Entropy of Fermi Liquids via Multidimensional Bosonization". *Phys. Rev. X* **2**, 011012 (2012).

[28] J. McMinis and N. M. Tubman. "Renyi entropy of the interacting Fermi liquid". *Phys. Rev. B* **87**, 081108 (2013).

[29] A. Kitaev and J. Preskill. "Topological Entanglement Entropy". *Phys. Rev. Lett.* **96**, 110404 (2006).

[30] M. Levin and X.-G. Wen. "Detecting Topological Order in a Ground State Wave Function". *Phys. Rev. Lett.* **96**, 110405 (2006).

[31] A. Hamma, R. Ionicioiu and P. Zanardi. "Bipartite entanglement and entropic boundary law in lattice spin systems". *Phys. Rev. A* **71**, 022315 (2005).

[32] A. Hamma, R. Ionicioiu and P. Zanardi. "Ground state entanglement and geometric entropy in the Kitaev model". *Physics Letters A* **337**, 22 – 28 (2005).

[33] J. von Neumann. "Beweis des Ergodensatzes und des H-Theorems in der neuen Mechanik". *Zeitschrift für Physik* **57**, 30–70 (1929).

[34] P. Bocchieri and A. Loinger. "Ergodic Foundation of Quantum Statistical Mechanics". *Phys. Rev.* **114**, 948–951 (1959).

[35] H. Tasaki. "From Quantum Dynamics to the Canonical Distribution: General Picture and a Rigorous Example". *Phys. Rev. Lett.* **80**, 1373–1376 (1998).

[36] S. Goldstein, J. L. Lebowitz, R. Tumulka and N. Zanghì. "Canonical Typicality". *Phys. Rev. Lett.* **96**, 050403 (2006).

[37] S. Popescu, A. J. Short and A. Winter. "Entanglement and the foundations of statistical mechanics". *Nature Physics* **2**, 754–758 (2006).

[38] A. Sugita. "On the Basis of Quantum Statistical Mechanics." *Nonlinear Phenom. Complex Syst.*. **10**, 192 (2007).

[39] P. Reimann. "Typicality for Generalized Microcanonical Ensembles". *Phys. Rev. Lett.* **99**, 160404 (2007).

[40] S. Sugiura and A. Shimizu. "Thermal Pure Quantum States at Finite Temperature". *Phys. Rev. Lett.* **108**, 240401 (2012).

[41] S. Sugiura and A. Shimizu. "Canonical Thermal Pure Quantum State". *Phys. Rev. Lett.* **111**, 010401 (2013).

[42] T. Kinoshita, T. Wenger and D. S. Weiss. "A quantum Newton's cradle". *Nature.* **440**, 900–903 (2006).

[43] S. Hofferberth, I. Lesanovsky, B. Fischer, T. Schumm and J. Schmiedmayer. "Non-equilibrium coherence dynamics in one-dimensional Bose gases". *Nature* **449**, 324 (2007).

[44] A. Polkovnikov, K. Sengupta, A. Silva and M. Vengalattore. "*Colloquium* : Nonequilibrium dynamics of closed interacting quantum systems". *Rev. Mod. Phys.* **83**, 863–883 (2011).

[45] M. Gring, M. Kuhnert, T. Langen, T. Kitagawa, B. Rauer, M. Schreitl, I. Mazets, D. A. Smith, E. Demler and J. Schmiedmayer. "Relaxation and Prethermalization in an Isolated Quantum System". *Science* **337**, 1318–1322 (2012).

[46] S. Trotzky, Y.-A. Chen, A. Flesch, I. P. McCulloch, U. Schollwöck, J. Eisert and I. Bloch. "Probing the relaxation towards equilibrium in an isolated strongly correlated one-dimensional Bose gas". *Nature Physics* **8**, 325–330 (2012).

[47] J. Eisert, M. Friesdorf and C. Gogolin. "Quantum many-body systems out of equilibrium". *Nature Physics* **11**, 124–130 (2015).

[48] O. Morsch and M. Oberthaler. "Dynamics of Bose-Einstein condensates in optical lattices". *Rev. Mod. Phys.* **78**, 179–215 (2006).

[49] R. Blatt and C. F. Roos. "Quantum simulations with trapped ions". *Nature Physics* **8**, 277–284 (2012).

[50] M. M. Wolf, F. Verstraete, M. B. Hastings and J. I. Cirac. "Area Laws in Quantum Systems: Mutual Information and Correlations". *Phys. Rev. Lett.* **100**, 070502 (2008).

[51] D. N. Page. "Average entropy of a subsystem". *Phys. Rev. Lett.* **71**, 1291–1294 (1993).

[52] S. W. Hawking. "Breakdown of predictability in gravitational collapse". *Phys. Rev. D* **14**, 2460–2473 (1976).

[53] S. K. Foong and S. Kanno. "Proof of Page's conjecture on the average entropy of a subsystem". *Phys. Rev. Lett.* **72**, 1148–1151 (1994).

[54] J. Sánchez-Ruiz. "Simple proof of Page's conjecture on the average entropy of a subsystem". *Phys. Rev. E* **52**, 5653–5655 (1995).

[55] S. Sen. "Average Entropy of a Quantum Subsystem". *Phys. Rev. Lett.* **77**, 1–3 (1996).

[56] C. Nadal, S. N. Majumdar and M. Vergassola. "Phase Transitions in the Distribution of Bipartite Entanglement of a Random Pure State". *Phys. Rev. Lett.* **104**, 110501 (2010).

[57] T. G. James R Garrison. "Does a single eigenstate encode the full Hamiltonian?" *arXiv* 1503.00729 (2015).

[58] T. Takayanagi and T. Ugajin. "Measuring black hole formations by entanglement entropy via coarse-graining". *Journal of High Energy Physics* **2010**, 54 (2010).

[59] T. Pálmai. "Excited state entanglement in one-dimensional quantum critical systems: Extensivity and the role of microscopic details". *Phys. Rev. B* **90**, 161404 (2014).

[60] L. Taddia, F. Ortolani and T. Pálmai. "Renyi entanglement entropies of descendant states in critical systems with boundaries: conformal field theory and spin chains". *Journal of Statistical Mechanics: Theory and Experiment* **2016**, 093104 (2016).

[61] M. B. Hastings, I. González, A. B. Kallin and R. G. Melko. "Measuring Renyi Entanglement Entropy in Quantum Monte Carlo Simulations". *Phys. Rev. Lett.* **104**, 157201 (2010).

[62] Y. Zhang, T. Grover and A. Vishwanath. "Entanglement Entropy of Critical Spin Liquids". *Phys. Rev. Lett.* **107**, 067202 (2011).

[63] T. Grover. "Entanglement of Interacting Fermions in Quantum Monte Carlo Calculations". *Phys. Rev. Lett.* **111**, 130402 (2013).

[64] R. Fan, P. Zhang, H. Shen and H. Zhai. "Out-of-time-order correlation for many-body localization". *Science Bulletin* **62**, 707 – 711 (2017).

[65] J. Maldacena, S. H. Shenker and D. Stanford. "A bound on chaos". *Journal of High Energy Physics* **2016**, 106 (2016).

[66] A. Kitaev. Talks in the 2015 Breakthrough Prize Fundamental Physics Symposium (2014) and the KITP Program "Entanglement in Strongly-Correlated Quantum Matter" (2015).

[67] P. Hosur, X.-L. Qi, D. A. Roberts and B. Yoshida. "Chaos in quantum channels". *Journal of High Energy Physics* **2016**, 4 (2016).

[68] T.-C. Lu and T. Grover. "Renyi Entropy of Chaotic Eigenstates". *arXiv* 1709.08784 (2017).

[69] R. Steinigeweg, J. Gemmer and W. Brenig. "Spin-Current Autocorrelations from Single Pure-State Propagation". *Phys. Rev. Lett.* **112**, 120601 (2014).

[70] Y. Yamaji, Y. Nomura, M. Kurita, R. Arita and M. Imada. "First-Principles Study of the Honeycomb-Lattice Iridates Na_2IrO_3 in the Presence of Strong Spin-Orbit Interaction and Electron Correlations". *Phys. Rev. Lett.* **113**, 107201 (2014).

[71] H. Ikeuchi, H. De Raedt, S. Bertaina and S. Miyashita. "Computation of ESR spectra from the time evolution of the magnetization: Comparison of autocorrelation and Wiener-Khinchin-relation-based methods". *Phys. Rev. B* **92**, 214431 (2015).

[72] R. Steinigeweg, J. Herbrych, X. Zotos and W. Brenig. "Heat Conductivity of the Heisenberg Spin-1/2 Ladder: From Weak to Strong Breaking of Integrability". *Phys. Rev. Lett.* **116**, 017202 (2016).

[73] M. Kawamura, K. Yoshimi, T. Misawa, Y. Yamaji, S. Todo and N. Kawashima. "Quantum lattice model solver H Φ". *Computer Physics Communications* **217**, 180 – 192 (2017).

[74] M. Suzuki. "Relationship between d-Dimensional Quantal Spin Systems and (d+1)-Dimensional Ising SystemsEquivalence, Critical Exponents and Systematic Approximants of the Partition Function and Spin Correlations". *Progress of Theoretical Physics* **56**, 1454–1469 (1976).

[75] E. Lubkin. "Entropy of an n-system from its correlation with a k-reservoir". *Journal of Mathematical Physics* **19**, 1028–1031 (1978).

[76] S. Lloyd and H. Pagels. "Complexity as thermodynamic depth". *Annals of Physics* **188**, 186 – 213 (1988).

[77] E. Lieb, T. Schultz and D. Mattis. "Two soluble models of an antiferromagnetic chain". *Annals of Physics* **16**, 407 – 466 (1961).

[78] I. Peschel. "Calculation of reduced density matrices from correlation functions". *Journal of Physics A: Mathematical and General* **36**, L205 (2003).

[79] A. Polkovnikov. "Microscopic diagonal entropy and its connection to basic thermodynamic relations". *Annals of Physics* **326**, 486 – 499 (2011).

[80] T. N. Ikeda, N. Sakumichi, A. Polkovnikov and M. Ueda. "The second law of thermodynamics under unitary evolution and external operations". *Annals of Physics* **354**, 338 – 352 (2015).

[81] M. A. Cazalilla. "Effect of Suddenly Turning on Interactions in the Luttinger Model". *Phys. Rev. Lett.* **97**, 156403 (2006).

[82] M. Rigol, V. Dunjko, V. Yurovsky and M. Olshanii. "Relaxation in a Completely Integrable Many-Body Quantum System: An *Ab Initio* Study of the Dynamics of the Highly Excited States of 1D Lattice Hard-Core Bosons". *Phys. Rev. Lett.* **98**, 050405 (2007).

[83] S. R. Manmana, S. Wessel, R. M. Noack and A. Muramatsu. "Strongly Correlated Fermions after a Quantum Quench". *Phys. Rev. Lett.* **98**, 210405 (2007).

[84] V. E. Hubeny, M. Rangamani and T. Takayanagi. "A covariant holographic entanglement entropy proposal". *Journal of High Energy Physics* **2007**, 062 (2007).

[85] T. Hartman and J. Maldacena. "Time evolution of entanglement entropy from black hole interiors". *Journal of High Energy Physics* **2013**, 14 (2013).

[86] P. Calabrese and J. Cardy. "Quantum quenches in extended systems". *Journal of Statistical Mechanics: Theory and Experiment* **2007**, P06008 (2007).

[87] P. Calabrese and J. Cardy. "Evolution of entanglement entropy in one-dimensional systems". *Journal of Statistical Mechanics: Theory and Experiment* **2005**, P04010 (2005).

[88] J. Cardy. "Thermalization and Revivals after a Quantum Quench in Conformal Field Theory". *Phys. Rev. Lett.* **112**, 220401 (2014).

[89] P. Calabrese and J. Cardy. "Quantum quenches in 1+1 dimensional conformal field theories". *Journal of Statistical Mechanics: Theory and Experiment* **2016**, 064003 (2016).

[90] J. M. Deutsch. "Quantum statistical mechanics in a closed system". *Phys. Rev. A* **43**, 2046–2049 (1991).

[91] M. Srednicki. "Chaos and quantum thermalization". *Phys. Rev. E* **50**, 888–901 (1994).

[92] M. Rigol, V. Dunjko and M. Olshanii. "Thermalization and its mechanism for generic isolated quantum systems". *Nature.* **452**, 854–858 (2008).

[93] J.-S. Caux and J. Mossel. "Remarks on the notion of quantum integrability". *Journal of Statistical Mechanics: Theory and Experiment* **2011**, P02023 (2011).

[94] M. Takahashi. *Thermodynamics of One-Dimensional Solvable Models*. Cambridge University Press (1999).

[95] B. Pozsgay. "The generalized Gibbs ensemble for Heisenberg spin chains". *Journal of Statistical Mechanics: Theory and Experiment* **2013**, P07003 (2013).

[96] F. H. L. Essler and M. Fagotti. "Quench dynamics and relaxation in isolated integrable quantum spin chains". *Journal of Statistical Mechanics: Theory and Experiment* **2016**, 064002 (2016).

[97] P. Barmettler, M. Punk, V. Gritsev, E. Demler and E. Altman. "Relaxation of Antiferromagnetic Order in Spin-1/2 Chains Following a Quantum Quench". *Phys. Rev. Lett.* **102**, 130603 (2009).

[98] M. Fagotti and P. Calabrese. "Evolution of entanglement entropy following a quantum quench: Analytic results for the XY chain in a transverse magnetic field". *Phys. Rev. A* **78**, 010306 (2008).

[99] V. Alba and P. Calabrese. "Entanglement and thermodynamics after a quantum quench in integrable systems". *Proceedings of the National Academy of Sciences* **114**, 7947–7951 (2017).

[100] C. K. Majumdar and D. K. Ghosh. "On Next-Nearest-Neighbor Interaction in Linear Chain. I". *Journal of Mathematical Physics* **10**, 1388–1398 (1969).

[101] P. R. Zangara, A. D. Dente, E. J. Torres-Herrera, H. M. Pastawski, A. Iucci and L. F. Santos. "Time fluctuations in isolated quantum systems of interacting particles". *Phys. Rev. E* **88**, 032913 (2013).

[102] P. Reimann. "Foundation of Statistical Mechanics under Experimentally Realistic Conditions". *Phys. Rev. Lett.* **101**, 190403 (2008).

[103] F. D. M. Haldane. "Exact Jastrow-Gutzwiller resonating-valence-bond ground state of the spin-1/2 antiferromagnetic Heisenberg chain with $1/r^2$ exchange". *Phys. Rev. Lett.* **60**, 635–638 (1988).

[104] B. S. Shastry. "Exact solution of an S=1/2 Heisenberg antiferromagnetic chain with long-ranged interactions". *Phys. Rev. Lett.* **60**, 639–642 (1988).

[105] T. Kiendl and F. Marquardt. "Many-Particle Dephasing after a Quench". *Phys. Rev. Lett.* **118**, 130601 (2017).

[106] P. Di Francesco, P. Mathieu and D. Senechal. *Conformal Field Theory*. Graduate Texts in Contemporary Physics. Springer-Verlag, New York (1997).

[107] W.-Z. Guo and S. He. "Rényi entropy of locally excited states with thermal and boundary effect in 2D CFTs". *Journal of High Energy Physics* **2015**, 99 (2015).

[108] D. Engelhardt. "Quench dynamics in confined 1 + 1-dimensional systems". *Journal of Physics A: Mathematical and Theoretical* **49**, 12LT01 (2016).

[109] G. Mandal, R. Sinha and T. Ugajin. "Finite size effect on dynamical entanglement entropy: CFT and holography". *arXiv:1604.07830* (2016).

[110] J. Maldacena. "The Large-N Limit of Superconformal Field Theories and Supergravity". *International Journal of Theoretical Physics* **38**, 1113–1133 (1999).

[111] X. Dong. "The gravity dual of Rényi entropy". *Nature Communications* **7**, 12472 (2016).

[112] S. Ryu and T. Takayanagi. "Holographic derivation of entanglement entropy from AdS/CFT". *Phys. Rev. Lett.* **96**, 181602 (2006).

[113] G. De Palma, A. Serafini, V. Giovannetti and M. Cramer. "Necessity of Eigenstate Thermalization". *Phys. Rev. Lett.* **115**, 220401 (2015).

[114] T. Mori and N. Shiraishi. "Thermalization without eigenstate thermalization hypothesis after a quantum quench". *Phys. Rev. E* **96**, 022153 (2017).

[115] V. Alba. "Eigenstate thermalization hypothesis and integrability in quantum spin chains". *Phys. Rev. B* **91**, 155123 (2015).

[116] G. Biroli, C. Kollath and A. M. Läuchli. "Effect of Rare Fluctuations on the Thermalization of Isolated Quantum Systems". *Phys. Rev. Lett.* **105**, 250401 (2010).

[117] L. D'Alessio, Y. Kafri, A. Polkovnikov and M. Rigol. "From quantum chaos and eigenstate thermalization to statistical mechanics and thermodynamics". *Advances in Physics* **65**, 239–362 (2016).

[118] S. D. Geraedts, R. Nandkishore and N. Regnault. "Many-body localization and thermalization: Insights from the entanglement spectrum". *Phys. Rev. B* **93**, 174202 (2016).

[119] L. Vidmar, L. Hackl, E. Bianchi and M. Rigol. "Entanglement Entropy of Eigenstates of Quadratic Fermionic Hamiltonians". *Phys. Rev. Lett.* **119**, 020601 (2017).

Acknowledgement

I would like to acknowledge my supervisor Masaki Oshikawa for giving me advices during five years of my graduate course. I also thank many collaborators: Hiroyuki Fujita, Shunsuke Furukawa, Tomonori Ugajin, Sho Sugiura, Thierry Giamarchi, Gábor Sárosi, Yuto Ashida, Yoshiki Fukusumi, Masataka Watanabe, and Ryohei Kobayashi. In addition, I would like to acknowledge following researchers for inspiring discussions: Ippei Danshita, Yohei Fuji, Shunsuke Furuya, Masamichi Miyaji, Soichiro Mohri, Yuki Nakaguchi, Tokiro Numasawa, Kiyomi Okamoto, Hiroaki Sumiyoshi, Yasuhiro Tada, Tadashi Takayanagi, and Shintaro Takayoshi. I express my gratitude to secretaries in our group, Atsuko Tsuji and Yuko Wada, for huge supports in paper-works about travels, grants, etc. Finally I would like to thank my parents for kind supports for my whole life, and I am also quite happy to thank Miki Hohkita for spending wonderful time with me.

During PhD course I have stayed at several institutes and universities. I would like to thank the Kavli Institute for Theortical Physics at University of California, Santa Barbara, the Yukawa Institute for Theoretical Physics at Kyoto University, and University of Geneva for their hospitality. I acknowledge Young Researchers' Exchange Program by the Japan Society for the Promotion of Science (JSPS) and the Swiss National Science Foundation.

I was supported by Advanced Leading Graduate Course for Photon Science (ALPS) of JSPS and by JSPS KAKENHI Grants No. JP16J01135. I acknowledge my sub-supervisors in ALPS: Professor Junji Yumoto and President Makoto Kuwata-Gonokami.